Diplomarbeit

2,6 GHz Radio Frequency Front End for Rapid Prototyping

ausgeführt zum Zwecke der Erlangung des akademischen Grades eines
Diplom-Ingenieurs unter Leitung von

Dipl.-Ing. Robert Langwieser
und
Ao. Univ.Prof. Arpad L. Scholtz
E389
Institut für Nachrichtentechnik und Hochfrequenztechnik

eingereicht an der Technischen Universität Wien
Fakultät für Elektrotechnik und Informationstechnik

von

Michael Fischer
9725775
Joh. Schmidtstr. 11, 3512 Mautern

Wien, Mai 2006

Abstract

In telecommunications a message has to be carried from one point to another. A transmitter is required at one end, while on the other end there is a receiver. If over the air transmissions are performed this typically happens using some carrier frequency.

This work describes the parameters of an RF (Radio Frequency) front end which can be used in rapid prototyping to augment an existing baseband processing unit to allow for transmissions at 2,6 GHz. Further one RF transmitter or RF receiver can be arranged with more uniform RF transmitters or RF receivers to allow for MIMO (Multiple Input Multiple Output) experiments.

The development of such an RF transmitter is described. An in-depth view of the components of the second upconversion stage is given. Last but not least several measurements are presented to certify the function of the transmitter and characterize it in the frequency domain, at different power levels, and with different modulation schemes.

Kurzfassung

Eine der Aufgaben der Nachrichtentechnik ist es, Information von einem Punkt zu einem zweiten zu transportieren. Ein Sender schickt die Nachricht ab, der Empfänger nimmt sie entgegen. Handelt es sich um Funkübertragung, geschieht dies in der Regel auf Trägerfrequenzebene.

Diese Arbeit beschreibt die Eigenschaften eines Hochfrequenz-Senders/Empfängers für eine bestehende Basisband-Einheit. Das Gesamtsystem kann dann für Übertragungen bei 2,6 GHz verwendet werden. Durch Zusammenschalten mehrerer gleichartiger Sender bzw. Empfänger können auch MIMO (Multiple Input Multiple Output) Übertragungen getestet werden.

Zuerst wird ein Überblick über die Entwicklung des Senders gegeben. Anschließend wird der Aufbau der zweiten Aufwärtsmischer-Stufe im Detail beschrieben. Zum Schluss werden Messungen des entwickelten Senders präsentiert. Sie beschreiben sein Verhalten im Frequenzbereich, bei verschiedenen Leistungen und unter verschiedenen Modulationsformaten.

Contents

1 Introduction **1**

2 System Concept **3**
2.1 Channel Sounding 3
2.2 Channel Emulation 4
2.3 Equipment Testing 5
2.4 MIMO Capability 5
2.5 Concept Summary 6
2.6 Remarks on the Baseband Processing Unit 7

3 Transmitter Concept **9**
3.1 Transmitter Features 9
3.1.1 Variable Output Power and Power Control 9
3.1.2 Adjustable Output Frequency 10
3.2 Overview of the Transmitter Components 10
3.3 The Transmitter RF Components 11
3.4 Transmitter Specification 12
3.5 Spectral Overview 13
3.6 Double Heterodyne Conversion Concept 14
3.7 PCB and Microstrip Line Properties 14

4 Transmitter Section "RF2600" **16**
4.1 "RF2600" Section Specification 17
4.2 Power Level Plan 17
4.3 Mixer 19
4.4 Image Rejection Filter 21
4.5 Buffer Amplifier 22
4.6 Switch 25
4.7 Transmitter Mode Output 26
4.7.1 Power Amplifier 27
4.7.2 Directional Coupler 27
4.7.3 Power Detector 28
4.8 Test Mode Output 30
4.8.1 Specification 30
4.8.2 Variable Attenuator 31
4.8.3 Power Detector 33
4.9 "RF2600" Section PCB 33

5 Performance Measurements **35**
5.1 Frequency Response 35
5.2 Output Power and Power Compression 40
5.3 Intermodulation 42
5.4 Harmonics and LO Drive Power 47
5.5 Error Vector Magnitude 50

6 Summary **56**

Acknowledgments **58**

Bibliography **59**

List of Abbreviations and Symbols **61**

List of Figures **63**

List of Tables **65**

Chapter 1

Introduction

In telecommunications one seeks to carry a message from one point to another. The message is either analogue, digital or a digitized version of an analogue signal. It is normally encoded in different ways before being transmitted. This is to ensure reliability, throughput, and safety of the message and adapt it to the transportation media. Possible ways of transport include – but are not limited to – over the air transmissions, electrical wires, or optical fibers.

If you want to design such a telecommunication system you have to measure your transportation media first to be able to make assumptions about it later. Everything between the transmitting and the receiving side is called the channel (see Figure 1.1). So one task is to find out something about the channel we have to deal with. This is called channel sounding.

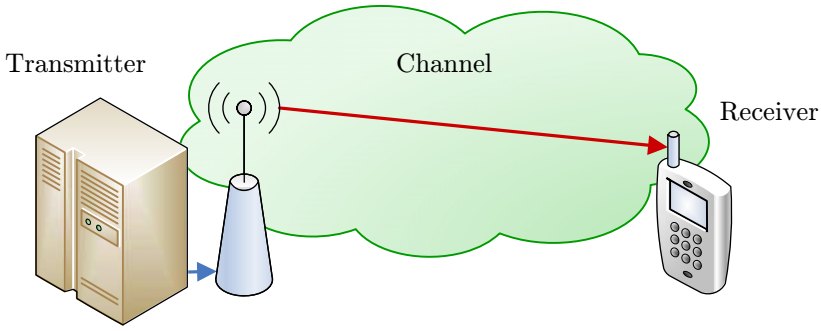

Figure 1.1: Typical telecommunication scenario.

Another task arises when you already know your channel and want to build telecommunication equipment for it. First you simulate both your device and the channel. After you have built your device you want to test it using a specific channel setup. To make this measurement reproducible and efficient a channel emulator is needed.

If you only have a receiver or a transmitter you need a reference transmitter or a reference receiver respectively to test your DUT[1]. This can be useful if you want to expose your DUT to different scenarios, to test it for compliance with a standard, or during production to ensure functionality and quality of function.

[1] Device Under Test

Traditionally, a signal is transmitted over a single antenna and received at another point with a single antenna. Nowadays antenna arrays and MIMO[2] becomes more and more important. You not only have a single transmission channel but several parallel ones using multiple transmitters, receivers, and antennas. The information is spread over these channels[3] using specially designed algorithms. The algorithms and their parameters depend on the assumptions you make of the channels and the information you obtained from them.

This work is dedicated to over the air transmissions or emulation of corresponding channels. The equipment described does not depend on a specific encoding technique or type of message. Hence this diploma thesis does not focus on a single transmission standard but stays on a more general level.

In this diploma thesis I will first illustrate the scenarios mentioned above in more detail. A flexible system concept will be introduced which can satisfy all of them. It consists of a baseband processing unit, an RF[4] transmitter, an RF receiver, and multiple local oscillators. These components will be described in Chapter 2.

In Chapter 3 I am going to describe the RF transmitter for 2,6 GHz used in this system. The transmitter is divided into two parts: a general upconverter to an intermediate frequency of 947,5 MHz, and a second section which performs the final upconversion.

The second part of the transmitter – called "RF2600" section – is the main part of my diploma thesis. It will be described in Chapter 4.

Chapter 5 presents measurement results of this RF section as well as of the complete transmitter.

Chapter 6 sums up the work of this diploma thesis and the results.

[2] Multiple Input Multiple Output

[3] An $m \times n$ MIMO system has not only $\max(m; n)$ channels but $m \cdot n$ although their parameters are normally not completely independent from each other.

[4] Radio Frequency

Chapter 2

System Concept

In this chapter I will introduce a system which serves several purposes:

- channel sounding
- channel emulation
- equipment testing
- MIMO capabilities

Such a system has to be flexible enough to adapt to these different requirements. In the following sections the objectives will be evolved and described in greater detail.

2.1 Channel Sounding

For channel measurements you need an RF source and an antenna to excite the channel on the first end. On the other end of the channel you need a second antenna and an RF receiver to receive the submitted data. This way you can calculate the parameters of the channel on the basis of the received data. All those components and their setup are shown in Figure 2.1.

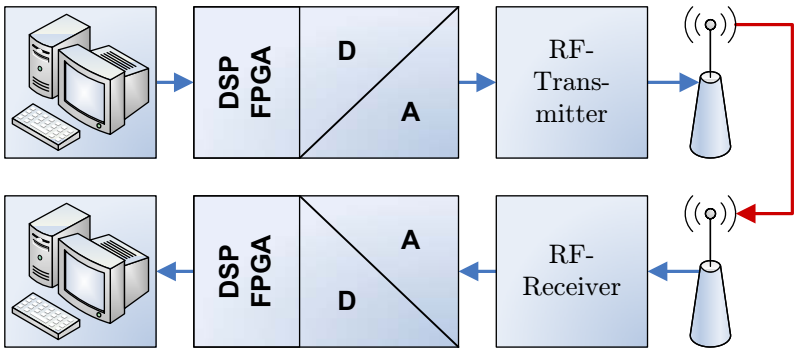

Figure 2.1: The RF front end used for channel sounding.

A DSP[1]/FPGA[2] block generates the signal. It is controlled by a regular computer. Although the signal is a complex baseband signal first, it is shifted to an intermediate frequency by digital upconversion. This intermediate frequency will be called f_{IF1} and is at 140 MHz. Further information will be given in Chapter 3. After this digital upconversion the signal is converted by a DAC[3] and placed at the analogue output of the baseband processing unit.

An RF transmitter unit converts the signal from its intermediate frequency up to the desired channel frequency. It is then transmitted via an antenna over the channel, received with a second antenna and downconverted in the receiver.

The output of the receiver is centered at the same intermediate frequency of 140 MHz. It is sampled with an ADC[4] and processed with another DSP/FPGA unit. The results are captured again using a regular computer system.

2.2 Channel Emulation

To test telecommunication equipment under different setups a channel emulator is needed. Such an emulator allows for fast changing and easily reproducible setups.

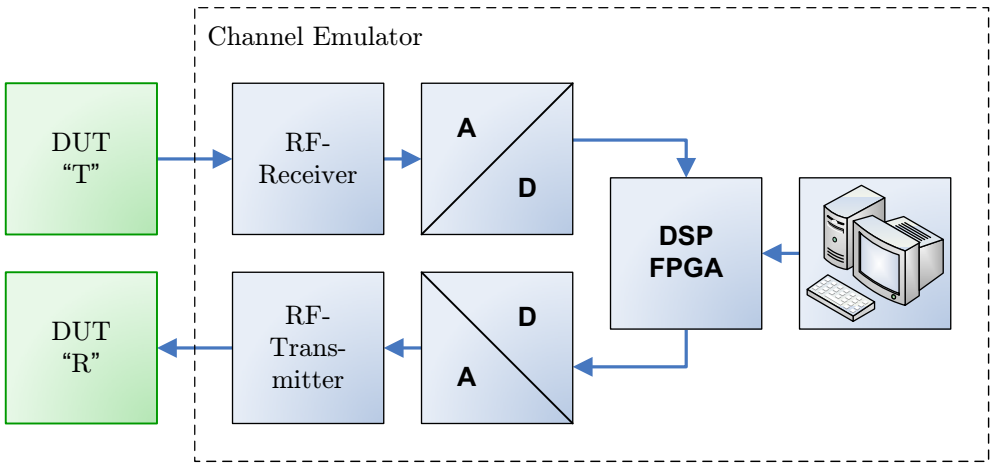

Figure 2.2: The RF front end used for channel emulation.

To evaluate the performance of a transmitter and a receiver (DUT "T" and DUT "R"), a setup as shown in Figure 2.2 can be used. In between those DUTs an RF receiver performs the downconversion of the received signal to a lower intermediate frequency f_{IF1}. At the intermediate frequency the signal is sampled and digitalized with an ADC. The channel is emulated via a DSP/FPGA unit

[1] Digital Signal Processor
[2] Field-Programmable Gate Array
[3] Digital to Analogue Converter
[4] Analogue to Digital Converter

which is controlled by a computer. The input signal to the transmitter is again generated by means of a DAC at an intermediate frequency f_{IF1}. The transmitter sees about the upconversion back to the RF frequency f_{RF}. This is the input signal to the DUT "R".

2.3 Equipment Testing

During development of a new telecommunication device normally only one side of a radio link is available or under development at a time. The other component has to be emulated by a flexible RF front end augmented with the right baseband processor. The setup used to emulate the transmitter or receiver can also accomplish emulating a channel to drive the DUT to its limits.

During production of telecommunication devices they have to undergo quality tests which ensure function and fulfillment of standards. This can not be achieved by – or can not be efficiently achieved by – simply setting up both sides of a radio link. In this case again one side has to be a flexible RF emulator. Figure 2.3 shows such a setup.

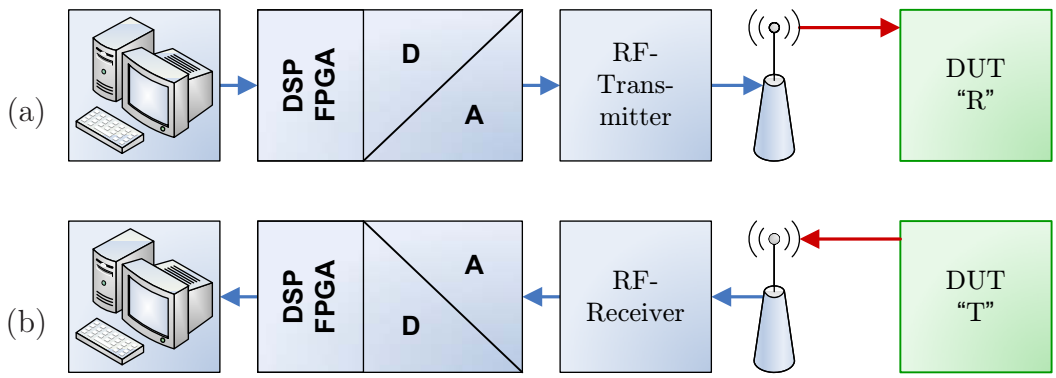

Figure 2.3: The RF front end used for test measurements.

The setup in Figure 2.3(a) emulates a transmitter with corresponding channel, while the setup shown in Figure 2.3(b) is the dual receiver emulator for an existing transmitter.

They consist of the same components introduced in Section 2.1. This time there is a device under test which is either directly connected to the transmitter or the signal is passed to it via an antenna close to it as shown in the figure.

2.4 MIMO Capability

All scenarios described above deal with a single channel. A possible expansion is to allow for multiple channels as needed for MIMO communications. Figure 2.4

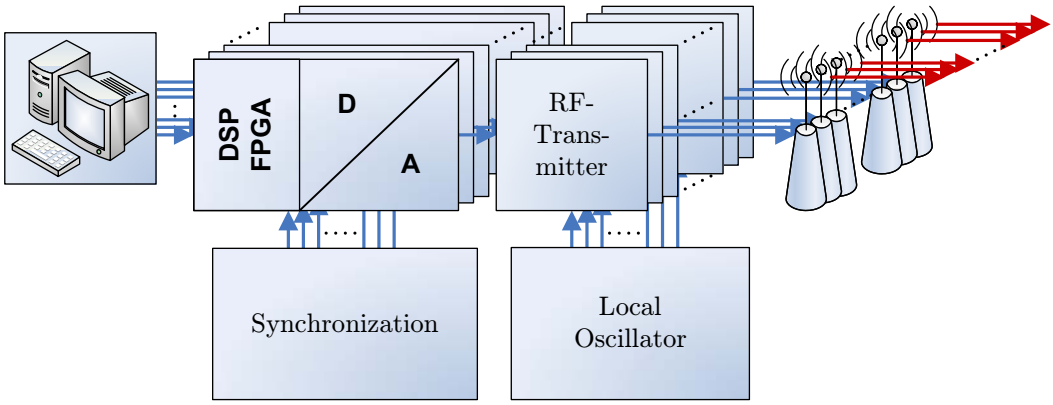

Figure 2.4: The RF front end used in MIMO applications.

shows such a scenario. Only a transmitter is depicted. The corresponding receiver can be easily constructed based on the components required for the transmitter.

The same components – as earlier described in Section 2.3 and Figure 2.3(a) – are shown. Here not only one baseband source and one RF transmitter are used but several. Both – baseband processing unit and transmitter – are built in a modular way and can be easily combined to a MIMO device. They share a local oscillator – or rather a set of local oscillators – which will be further explained in Chapter 3.

If the signals at the intermediate frequency f_{IF1} are synchronized and the RF transmitters are fed by local oscillators with the same frequency and phase then the input signals to the RF transmitters are in phase and this will not be lost at the outputs. Several antennas can be supplied with signals and allow for true MIMO experiments or measurements. In the following chapters I will only discuss a single channel without loosing the aspects necessary for MIMO capability.

2.5 Concept Summary

Figure 2.5 shows the complete setup. A computer controls the baseband processing unit. If more baseband processing units are used in a MIMO setup, up to eight of them can be combined in a single 19" case to ease handling and power supply. Then a separate device synchronizes them.

The upper two devices form the RF front end. Each transmitter unit is responsible for one antenna. Again eight units can be combined in one 19" housing. As will be explained in Chapter 3 two local oscillators are needed for the upconversion. Each of these synthesizers is followed by a 8-times power splitter. So one local oscillator device can be used for eight transmitters.

Each connection shown in Figure 2.5 actually is not a single connection but can be multiple parallel connections for different antennas. Of course the single antenna symbol shown is then multiple physical antennas or connections to the

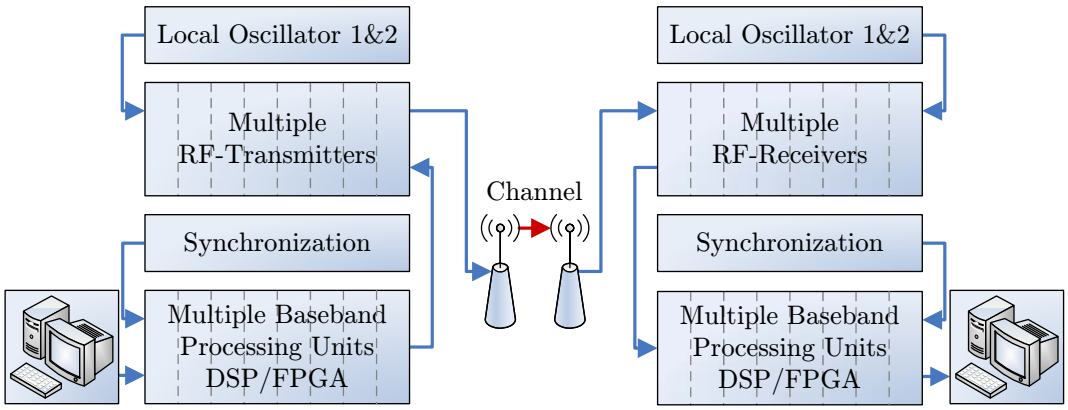

Figure 2.5: The complete system.

receiver side. In the standard configuration each of the 19" baseband and transmitter housings holds up to eight units as explained above. This can be extended by using another set of transmitters and baseband processing units. Synchronization unit and local oscillators can be extended respectively. This allows for up to $8 \times 8 = 64$ antennas on the transmitter side.

On the right side of the figure the whole processing runs in the opposite direction. Multiple antennas are connected to multiple receivers. Again there can be between a single and 64 antennas. The baseband processing units are of the same kind as the one used on the transmitter side.

2.6 Remarks on the Baseband Processing Unit

The baseband processing unit used in the scenarios described above is sometimes shown as a signal source or a receiver at the intermediate frequency f_{IF1}. It actually consists of a ADC, a DSP/FPGA unit to perform the digital processing, and a DAC as shown in Figure 2.6.

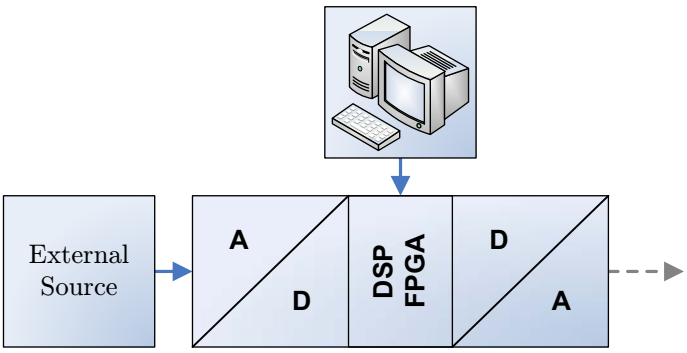

Figure 2.6: The complete baseband processing unit.

When used as a signal source it can generate a signal by means of the DAC.

In a different setup it is used to sample an external source. This data then can be altered in any way – e.g. similar to a channel emulator – before it is converted back to an analogue signal by the DAC.

The baseband processing unit is controlled and supervised by a computer. Since the RF front end has several adjustment and setup parameters as well, those can either be controlled by the same computer or by means of the baseband processing unit.

The RF front end does not depend on the baseband processing unit but can be operated autarkic. An external signal source with an output at the first intermediated frequency f_{IF1} is sufficient. It can be directly connected to the input of the RF transmitter. The same is true for the receiver side. Actually all measurements presented in Chapter 5 have been taken without the baseband processing unit but with standalone signal generators.

Chapter 3

Transmitter Concept

In Chapter 2 a concept for a system was introduced which allows for flexible RF measurements or channel emulations. It consists of a baseband processing unit working at a low intermediate frequency and an RF front end. The RF front end falls apart into three different units: a transmitter, a receiver and a local oscillator unit.

This diploma thesis focuses on the transmitter. The transmitter has different purposes. To fulfill them and to be more flexible a double heterodyne conversion concept was chosen. In this chapter a general concept for the complete transmitter will be presented. Chapter 4 then describes the section of the transmitter which performs the second upconversion.

3.1 Transmitter Features

To be flexible enough the transmitter offers the following features:

- variable output power between −90 dBm and +13 dBm
- transmitter and test mode output
- output power control loop
- adjustable output frequency (±100 MHz and in bands)
- double heterodyne conversion

3.1.1 Variable Output Power and Power Control

There are two outputs. One acts as a transmitter mode output with a maximal power level of +13 dBm. Internally the signal power can be attenuated two times by up to 30 dB, resulting in a minimal output power of −47 dBm. This output can be directly connected to an antenna to allow for over the air transmissions.

The second output offers −10 dBm maximal power, but has a third 30 dB variable attenuator. The minimum power level for this output is therefore below −90 dBm.

At each of the two outputs there is a power detector which supplies feedback to the variable attenuators via a micro controller. This control loop leads to a well regulated output power.

The variable attenuators are located before and after each upconverting mixer. This minimizes the crosstalk since the attenuation happens at different frequencies and results in good isolation even at high attenuator levels.

3.1.2 Adjustable Output Frequency

The transmitter is designed to accept input at an intermediate frequency f_{IF1} of 140 MHz. By means of double heterodyne conversion the final radio frequency f_{RF} is reached. This method requires two local oscillators. The first operates at a fixed frequency. The second one can be tuned in a range of about ±100 MHz. This allows to select the required output center frequency f_{RF} by means of the second local oscillator.

If another output frequency band is required only the second upconversion stage has to be redesigned. The first stage – called 1 GHz section – is left unchanged. The result is a selectable output frequency – in bands. Since the second stage – called "RF2600" section – is located on a different PCB[1] it can even be replaced at a later time.

3.2 Overview of the Transmitter Components

The transmitter consists of several logical and physical sections. This is illustrated in Figure 3.1.

Two different PCBs are mounted atop of each other. The first has approximately euro card format[2]. This allows for easy vertical mounting in a standard 19" housing with 3U height[3]. It carries the first upconversion stage from the low intermediate frequency f_{IF1} to the higher second intermediate frequency f_{IF2} with nearly 1 GHz. This will be explained in the next section.

Besides the first upconversion this base PCB has to fulfill other duties as well. A micro controller is located near the right edge. It is a MSP430F169 from Texas Instruments. Its purpose is to control the individual components on the RF path like the variable attenuators (Section 4.8.2) or select the output port (sections 4.6 and 4.7.1). It also receives the analogue DC[4] measurement signals from the power detectors (Section 4.7.3). On the other side it has a serial interface to the baseband processing unit or a separate computer. Last but not least it

[1] Printed Circuit Board
[2] 160 mm × 100 mm
[3] 1U = 44,45 mm
[4] Direct Current

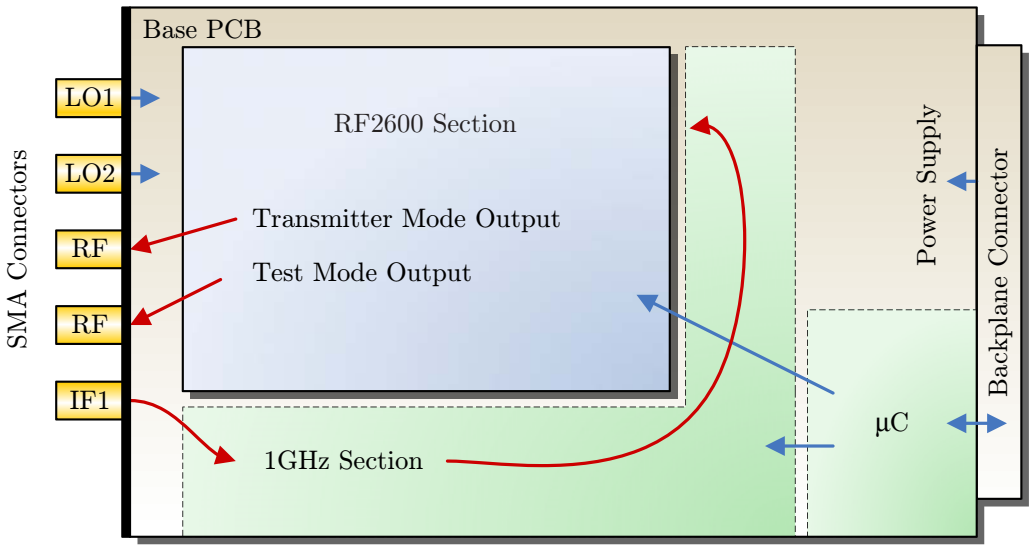

Figure 3.1: Overview of the transmitter components.

controls status LEDs[5] on the front panel to indicate the active output and the transmitter status to the user.

At the left side of the base PCB there are five SMA[6] RF connectors to the front panel. On the right side there is a multipin connector to the back plane. This connector carries the transmission lines of the micro controller to the rear panel as well as is the power supply input. Four different voltages are available: ±12 V, and ±5 V.

The second PCB takes care of the second upconversion to the final RF frequency f_{RF}. The purpose of this PCB is the topic of Chapter 4.

3.3 The Transmitter RF Components

The so far presented features result in a structure as shown in Figure 3.2. It shows the two upconversion stages. After each mixer there is a bandpass filter which suppresses the components at the image frequency as well as of the remaining input signal, local oscillator and its harmonics. At the input to the transmitter another filter is needed since the signal coming from the baseband processing unit still carries its harmonics from the digital to analogue conversion done at the end of the signal chain in the baseband processing unit.

At the end of the diagram you can see the switch and the two outputs explained in Section 3.1.1. About the right half of the figure is delimited with a dashed line. This is the "RF2600" section which is the main work of this diploma thesis and will be explained in Chapter 4. Not shown in the figure are the variable

[5] Light Emitting Diodes
[6] SubMiniature version A (connector)

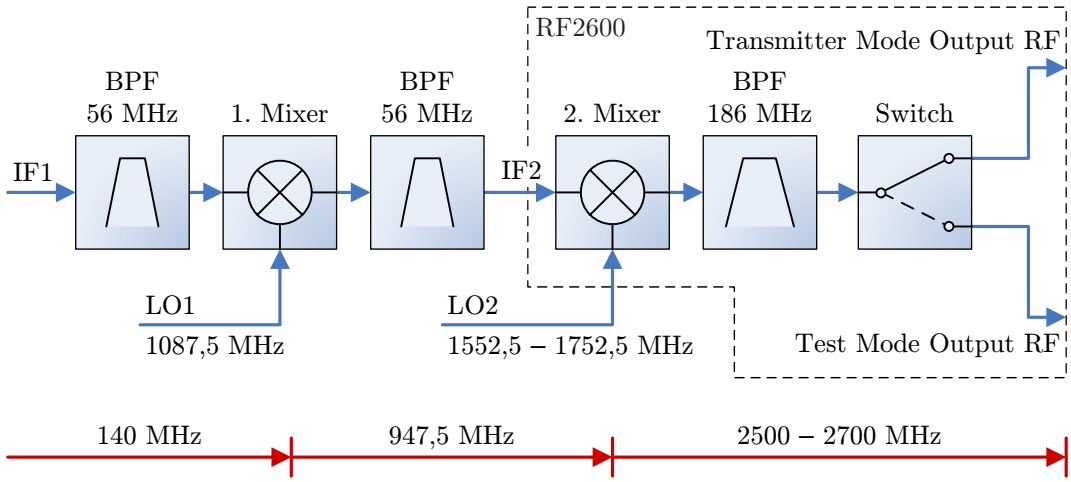

Figure 3.2: Block diagram of the transmitter.

attenuators and the necessary buffer and power amplifiers. They will be presented and discussed in Chapter 4 as far as they are part of the "RF2600" section.

3.4 Transmitter Specification

The transmitter discussed in this diploma thesis operates at a nominal output frequency of 2,6 GHz. It expects its input signal at the intermediate frequency f_{IF1} of 140 MHz. After two upconversions the output frequency f_{RF} is between 2500 and 2700 MHz.

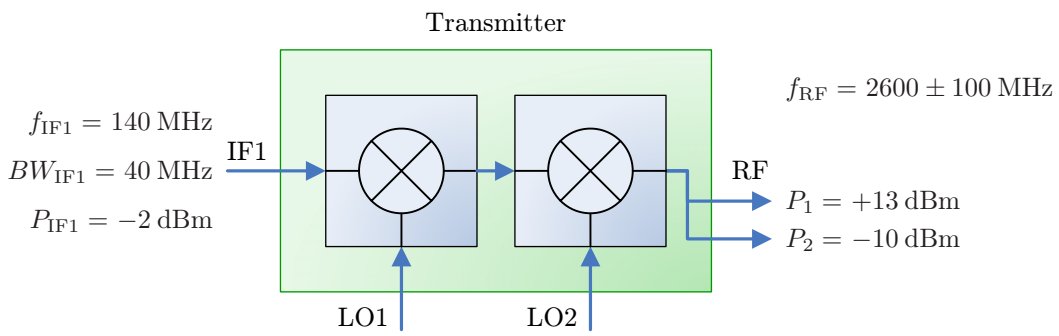

Figure 3.3: Specification of the transmitter.

Figure 3.3 gives a graphical representation of the specification of the transmitter. At the input the maximal signal bandwidth specified is 40 MHz. After the input there is a bandpass filter with a 3 dB bandwidth of 56 MHz as can be seen in Figure 3.2. This filter sets the actual 3 dB bandwidth of the system. The nominal input power level is −2 dBm.

The specification for the output is obtained by combining the features presented in Section 3.1. This includes the output frequency and frequency range and the power levels for each of the two outputs.

3.5 Spectral Overview

The input signal to the transmitter is centered at 140 MHz as specified in Figure 3.3 and illustrated in Figure 3.4(a) on the left. As explained above there are two local oscillators. The first one LO1 resides at 1087,5 MHz. After the frequency conversion of IF1 by means of LO1, this results in a lower sideband around 947,5 MHz and an upper sideband around 1227,5 MHz. The upper sideband is suppressed by the first image rejection filter. The lower sideband is passed with a bandwidth of 56 MHz. This is the input to the "RF2600" section at the second intermediate frequency f_{IF2} as shown in Figure 3.4(b).

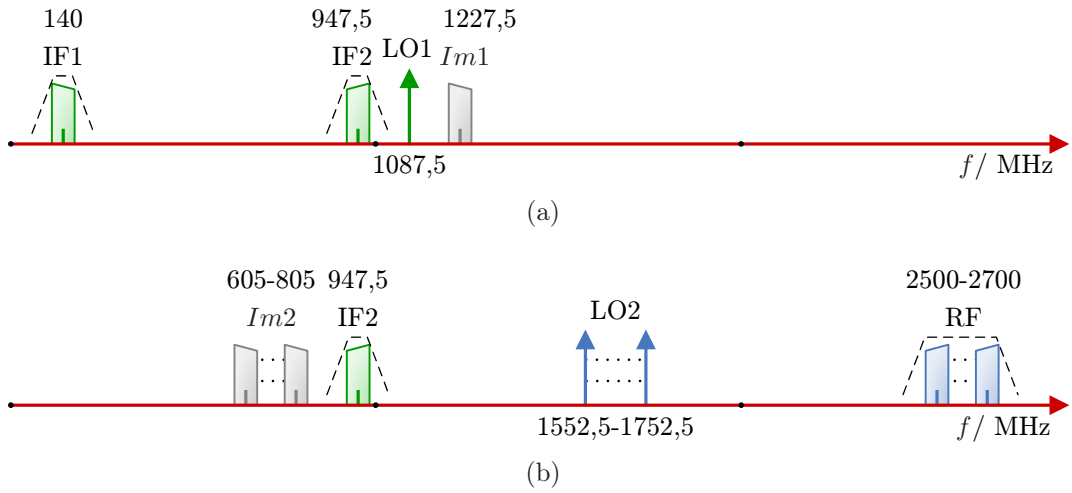

Figure 3.4: Spectral overview of the transmitter.

The second local oscillator LO2 is variable. It is allowed to be set anywhere between 1552,5 and 1752,5 MHz minus half the bandwidth of the input signal. Again after the mixing process a lower and an upper sideband arise. This time there is no specified constant center frequency since the LO2 is not fixed. Figure 3.4(b) takes this into account and shows the sidebands based on the minimal and maximal LO2 frequency. This time the upper sideband is allowed to pass the second image rejection filter. This transmit filter has a bandwidth of 200 MHz.

In agreement with Figure 3.4 the final output signal is a spectrally inverted and shifted version of the input signal. The inversion is a result of first letting the lower and then the upper sideband pass the BPFs[7]. This is no problem since it can easily be compensated for in the baseband processing unit.

[7] Band Pass Filters

3.6 Double Heterodyne Conversion Concept

One can perform a single conversion from the low intermediate frequency f_{IF1} of 140 MHz to the final output frequency f_{RF} between 2500 and 2700 MHz. A low side local oscillator with $f_{\mathrm{LO}} = 2460$ MHz is needed to achieve an upper sideband at 2600 MHz. The lower sideband is then at $f_{Im} = 2320$ MHz. At the output of the mixer there is also the crosstalk from the local oscillator input. The distance between f_{Im} and f_{RF} is approximately $1/6^{\mathrm{th}}$ of an octave and $1/13^{\mathrm{th}}$ of an octave for f_{LO} and f_{RF}. An image rejection filter has to suppress both the lower sideband and the remaining local oscillator at these short distances.

Further more the output should not be fixed but tunable between 2500 and 2700 MHz. The local oscillator needs a tuning range of 200 MHz which would result in a frequency f_{LO} from 2360 to 2560 MHz. This overlaps with the output frequency range. A suitable transmit filter is not possible for this arrangement. Similar figures are obtained if a high side LO[8] is used from 2640 to 2840 MHz.

If a double heterodyne conversion concept is chosen as illustrated in sections 3.4 and 3.5, there is a second intermediate frequency f_{IF2} at $947,5$ MHz with a first LO at $f_{\mathrm{LO1}} = 1087{,}5$ MHz. This time the distances between f_{IF2} and the undesired outputs of the mixer f_{Im1} and f_{LO1} are larger: approximately $1/3^{\mathrm{rd}}$ and $1/5^{\mathrm{th}}$ of an octave respectively. Image rejection filters with sufficient suppression in this distances are more easily available. Since the first local oscillator can now be at a fixed frequency there is no longer a problem with overlap.

At the second upconversion the distance between local oscillator LO2 and the upper sideband at f_{RF} is now 947,5 MHz which is more than one half of an octave. Transmit filters with 200 MHz bandwidth and reasonable suppression at those frequencies are again better obtainable. Furthermore only the second upconversion stage has to be redesigned if there is need for another output frequency. This has already been mentioned in Section 3.1.2.

3.7 PCB and Microstrip Line Properties

In Section 3.2 I described the assignment of the components to the two PCBs and their arrangement. Both PCBs are made of a substrate called FR4. FR4 is an industry standard substrate and can be handled by any PCB manufacturer. However the RF properties of FR4 – especially its relative permittivity ε_r – are not standardized and differ from manufacturer to manufacturer. It still can be used for frequencies below 3 GHz.

The main parameters of two different version of FR4 are given in Table 3.1. The first upconversion stage and the micro controller are located on FR4 with 1,6 mm thickness. It is mechanically stronger than FR4 with only 0,8 mm thickness and suited for direct insertion into the 19" housing.

[8] Local Oscillator

Table 3.1: Parameters of the PCB substrate FR4.

Parameter	FR4 0,8	FR4 1,6	Unit
Substrate thickness h	0,8	1,6	mm
Relative permittivity ε_r	$4{,}4 \div 4{,}7$	$4{,}4 \div 4{,}7$	
Dielectric loss tangent $\tan\delta$	0,014	0,014	
Copper plating thickness	35	35	μm
Copper resistivity	1,673	1,673	$\mu\Omega$ cm
50 Ω microstrip line width w for 2,6 GHz	1,4	2,9	mm

The second upconversion is done on a different PCB (again see Section 3.2). This time the thinner substrate FR4 0,8 is used. Great mechanical strength is not necessary since the PCB is smaller and mounted on the base PCB. The main advantage however is the reduced width of 50 Ω microstrip lines.

As transmission lines for the RF signals microstrip lines where chosen (see [1] ch. 4.8, [2], [3] ch. 3-8, or [4] ch. 4.8). They require a continuous ground plane on one side and a simple flat conductor with sufficient clearance on the other side as illustrated in Figure 3.5. The ground plane is only interrupted for connections carrying DC signals. For RF signals the characteristic impedance Z_w of the transmission line is of great relevance. Z_w is mostly dependant on the height of the substrate h, the dielectric behavior given by its relative permittivity ε_r, and the width of the microstrip line w. Since two of these parameters are already determined by the chosen substrate, Z_w can only be selected by varying the width w.

The inputs and outputs as well as all components of the transmitter have been matched to 50 Ω. I calculated the appropriate line width of a 50 Ω microstrip line with RF simulation software tools. The results are given in Table 3.1.

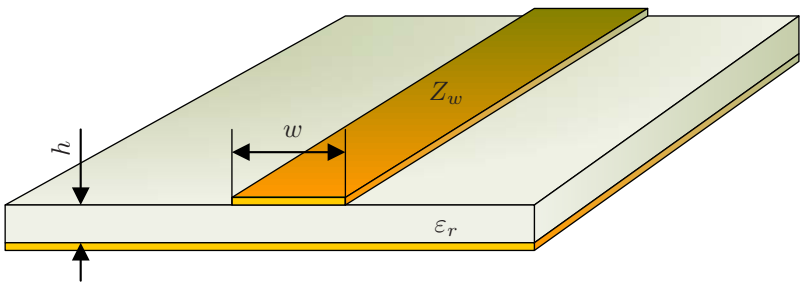

Figure 3.5: Parameters of microstrip lines.

Chapter 4

Transmitter Section “RF2600”

As previously stated the transmitter described in Chapter 3 consists of two analogue sections. The second upconversion and final amplification is done in the “RF2600” section which will be described in this chapter.

Figure 4.1 gives a more detailed overview than Figure 3.2. The second upconverter stage and the two output branches can again be seen. Moreover the gain and attenuation blocks are shown.

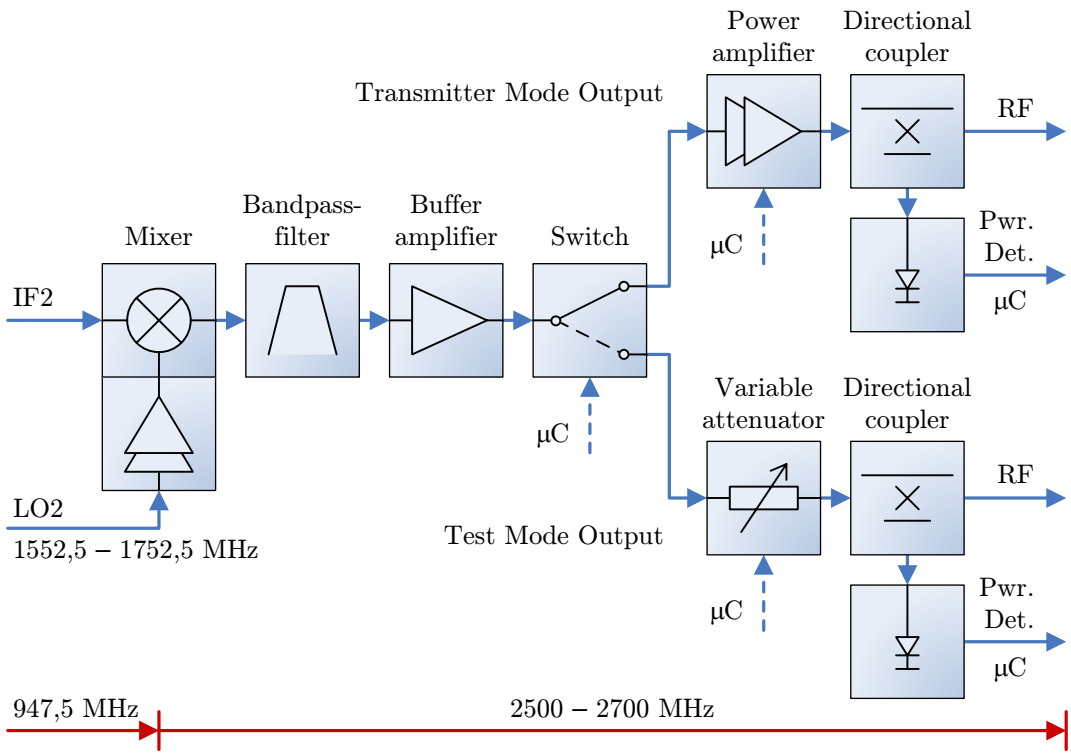

Figure 4.1: Overview of the “RF2600” section.

4.1 "RF2600" Section Specification

To keep the development of transmitters at different output frequencies flexible, only the second upconverter stage has to be redesigned. The interface between first and second section is therefore clearly specified. This is illustrated in Figure 4.2.

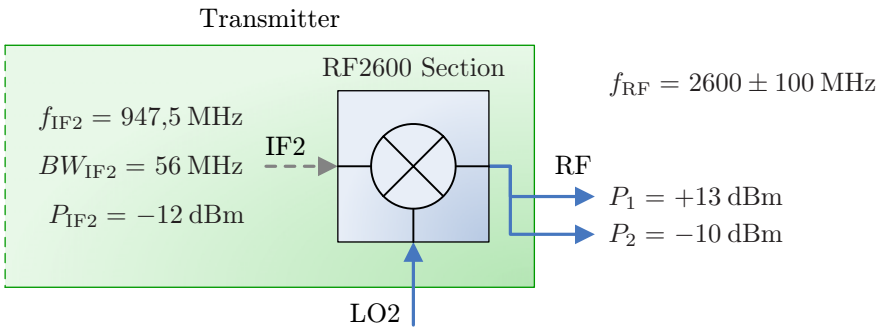

Figure 4.2: Specification of the "RF2600" section.

An arbitrary signal with 56 MHz bandwidth centered at 947,5 MHz has to be transformed to a higher center frequency in the range of 2,5 to 2,7 GHz. Strictly speaking the signal at the IF1 input has only 40 MHz bandwidth. On the other hand all filters in the 1 GHz section have a bandwidth of 56 MHz. That is why here this bigger bandwidth is given. The exact center frequency is determined by the second external local oscillator. Depending on the actual input bandwidth it can extend to the limits of 2600 ± 100 MHz. Hence the bandwidth of the transmit filter is given as 200 MHz.

As presented in Chapter 3 two outputs with different power levels and capabilities allow for a flexible use of the transmitter. The low power test mode output even possesses an extra variable attenuator.

Both outputs have a connection to a micro controller. A directional coupler shown in Figure 4.1 branches off a proportional amount of power. A subsequent power detector converts the RF power to a DC voltage which is then measured by the micro controller ("Pwr. Det." in Figure 4.1). Then the micro controller can control the variable attenuators of the first and second transmitter section.

4.2 Power Level Plan

Before any earnest design steps can be performed, a power level plan has to be developed. It is given in Table 4.1. I started with the specified data given in Figure 4.2 in the first line of the table. Each following line gives the data for one of the components of the "RF2600" section.

The objective is to reach the required output parameters given in Figure 4.2. For the transmitter mode output the power level plan is documented in Table 4.1,

while the test mode output is addressed in Table 4.4.

The first column of Table 4.1 gives the center frequency f_c. As mentioned above, for the components after the mixer no exact center frequency can be given since it is variable and determined by the second external local oscillator.

Every component is then characterized by its gain G and noise figure F. In most cases the maximum gain was first considered and later replaced by an actually measured value. The noise figure F is a measure for the degradation in the SNR[1] between the input and output of the component ([1] ch. 11.1).

$$F = \frac{SNR_{in}}{SNR_{out}} = \frac{P_{in}/N_{in}}{P_{out}/N_{out}}, \tag{4.1}$$

where P_x is the power of the desired signal while N_x is the undesired noise power. Noise figures had not been available for each component. Since an attenuator with a gain of $-x$ dB has a noise figure of x dB the third column was replenished with these values for passive components.

Table 4.1: Power level plan for the "RF2600" section.

Component	f_c MHz	G dB	F dB	P dBm	F_{total} dB
Input IF2	947,5			-12,0	
Attenuator	947,5	-0,2	0,2	-12,2	0,2
Balun	947,5	-0,8	0,8	-13,0	1,0
Mixer	2600	-0,5	13,0	-13,5	14,0
Balun	2600	-3,0	3,0	-16,5	14,2
BPF	2600	-1,0	1,0	-17,5	14,4
Buffer amplifier	2600	14,5	1,2	-3,0	14,5
Switch	2600	-1,5	1,5	-4,5	14,5
Attenuator	2600	-1,5	1,5	-6,0	14,5
Power amplifier	2600	22,0	4,0	16,0	14,6
BPF	2600	-1,0	1,0	15,0	14,6
Directional coupler	2600	-2,0	2,0	13,0	14,6
Output transmitter mode	2600			13,0	

The forth column gives the power level at the output of every component. It has to be taken into consideration as the input power of the following component. Too low power degrades the SNR, whereas too high power drives a component into compression, saturation, or even causes damage.

For each component a presumed noise power level was calculated. It is not given here. Instead the fifth column states the cumulative noise figure F_{total}.

[1] Signal Noise Ratio

This is calculated using Friis' formula (see [5] ch. 8.2),

$$F_{1,n} = F_1 + \frac{F_2 - 1}{G_1} + \frac{F_3 - 1}{G_1 G_2} + \cdots + \frac{F_n - 1}{G_1 G_2 \cdots G_{n-1}}, \tag{4.2}$$

where F_i and G_i are the individual noise figures and gains of each of the components. After the high noise figure of the mixer the subsequent components do not contribute significantly to the overall noise figure any more.

Figure 4.3 shows a graphical representation of the power P for both the transmitter and the test mode output. The power for the transmitter mode output power starts at -12 dBm on the left. It decreases with every component up to the BPF. The buffer amplifier increases the power again. After the switch the plot splits into two sections. The dashed plot represents the test mode output path. Its data is shown in Table 4.4. The top plot shows the cumulative noise figure for the transmitter mode output. The data for the noise figure of the test mode output is not plotted since it is almost identical as can be seen in Table 4.4.

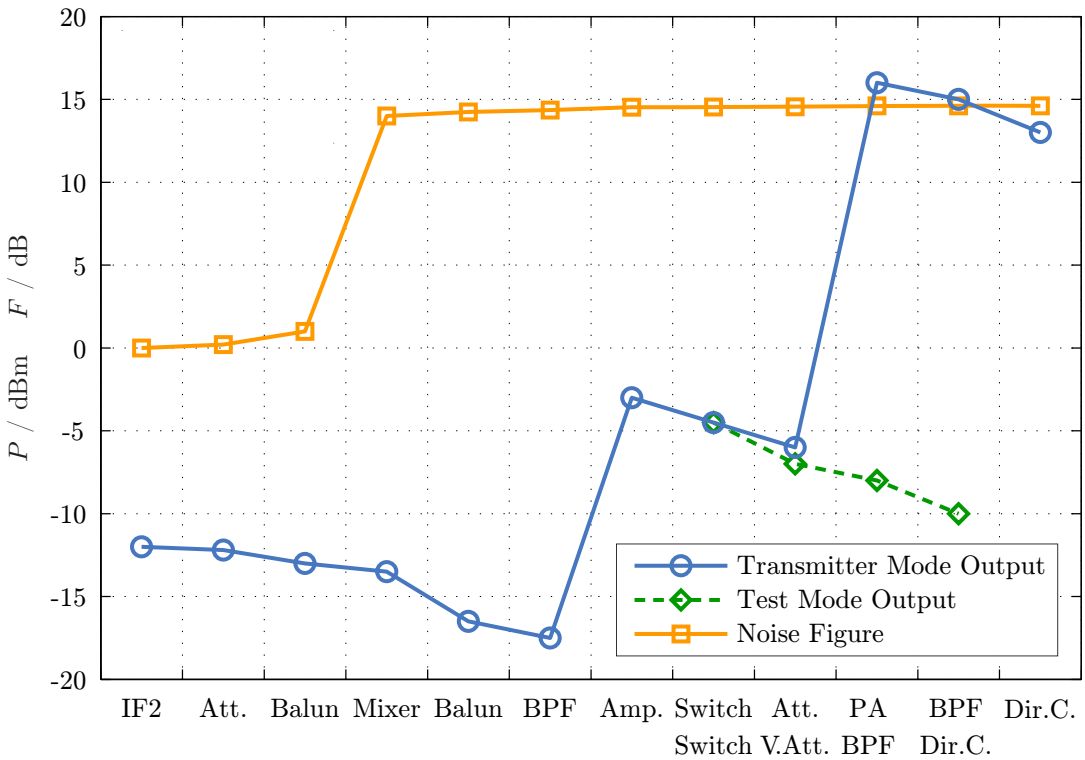

Figure 4.3: Power level diagram for the "RF2600" section.

4.3 Mixer

The mixer is one of the central elements of the second upconverter stage. It multiplies the input signal IF2 centered at the second intermediate frequency of

947,5 MHz with the second local oscillator LO2 ([5] ch. 11)

$$\begin{aligned} x_{out}(t) &= x_{\mathrm{IF2}}(t)\; x_{\mathrm{LO2}}(t) \\ \text{with} \quad x_{\mathrm{LO2}}(t) &= \cos(\omega_{\mathrm{LO2}}\, t) = \cos(2\pi\, f_{\mathrm{LO2}}\, t)\ . \end{aligned} \tag{4.3}$$

While x_{IF2} carries the information, x_{LO2} is a purely sinusoidal signal. At the output we obtain the same spectral information shifted to the sum and the difference frequencies of IF2 and LO2 (see Figure 3.4(b)). If x_{IF2} is also of the form $\cos(2\pi\, f_{\mathrm{IF2}}\, t)$ the result can be written as

$$x_{out}(t) = \frac{1}{2}\Big[\cos\Big(2\pi\,(f_{\mathrm{LO2}} + f_{\mathrm{IF2}})\, t\Big) + \cos\Big(2\pi\,(f_{\mathrm{LO2}} - f_{\mathrm{IF2}})\, t\Big)\Big]. \tag{4.4}$$

This leads us to

$$f_{\mathrm{RF}} = f_{\mathrm{LO2}} + f_{\mathrm{IF2}} \qquad \text{and} \qquad f_{Im2} = f_{\mathrm{LO2}} - f_{\mathrm{IF2}}\,. \tag{4.5}$$

In Figure 4.4 you can see a detailed block diagram of this part of the "RF2600" section.

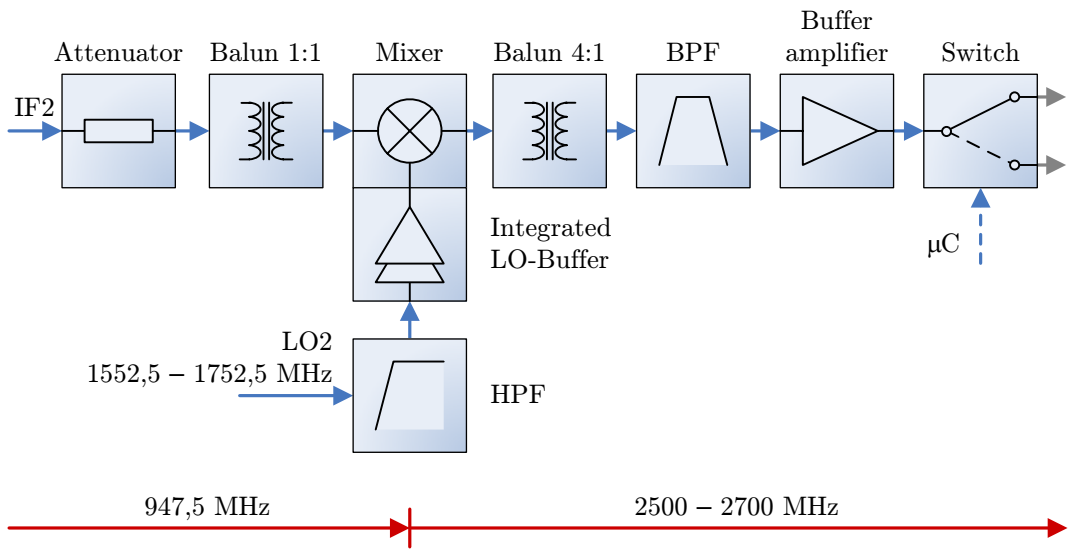

Figure 4.4: Overview of the second upconverter stage.

The signal at the sum frequency f_{RF} around 2,6 GHz is the desired output signal (RF in Figure 3.4(b)). At the difference frequency around 705 MHz lies the image frequency f_{Im2}. It is suppressed by a bandpass filter that will be described in Section 4.4.

For the mixer I chose the LT 5521 by Linear Technology [6]. As can be seen in Figure 4.4 it has an integrated buffer amplifier for the local oscillator input. It has differential inputs and outputs. Therefore BALUNs[2] are needed. The transformer at the output is also used as an 4:1 impedance converter.

[2] BALanced - UNbalanced converters

The local oscillator is located in a separate device. At its output it has a lowpass filter for suppression of harmonics. On the input of the "RF2600" section there is another filter. Some part of the IF2 input signal still exists at the LO2 input. To further decrease this undesired fraction and therefore increase the isolation between IF2 and LO2 input there is this second filter: a highpass filter. It helps to decrease the crosstalk from one transmitter board to another one or a receiver which is connected to the same local oscillators. This results in better decoupling of two channels. The HPF[3] can be seen in Figure 4.4.

In front of the mixer I placed an attenuator. It is a Π-style type which can be easily short circuited with an 0 Ω resistor when not needed. Its purpose is to allow for power level adjustment in order to fulfill the requirements of the subsequent components.

To check the figures given in the data sheet [6] a test PCB was built and assembled (see figures 4.5(a) and 4.5(b)). The whole block – consisting of the two transformer BALUNs and the mixer – has an insertion loss of 3,2 dB and its 0,1 dB compression point is at 6,4 dBm input power. The IF2 band is suppressed by 17 dB, the LO power and the power of its 2nd harmonic are −48 dBm and −12 dBm respectively at the output.

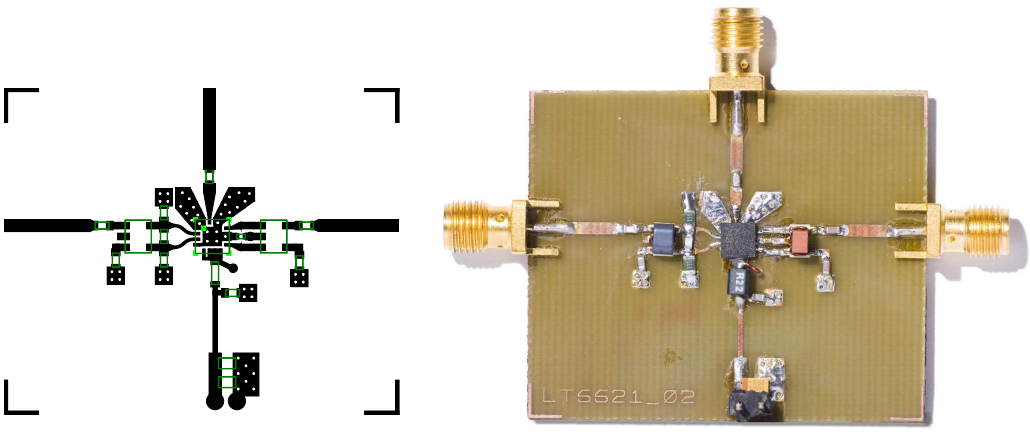

(a) (b)

Figure 4.5: Layout with part outlines and assembled test PCB of the mixer.

4.4 Image Rejection Filter

After the mixer there are several frequency components. The desired radio frequency band f_{RF}, the image frequency f_{Im2}, a not well suppressed local oscillator f_{LO2}, as well as further undesired harmonics of the intermediate frequency and LO1 and LO2 (see also the measurements described in Section 5.4). The im-

[3] High Pass Filter

age rejection filter is a bandpass filter designed to suppress all those undesired components.

I chose a 3-pole dielectric cavity filter from NTK [7]. Its frequency response can be seen in figures 4.6(a) and 4.6(b). It has a low insertion loss of only 1,0 dB and a 3 dB bandwidth of 197 MHz around its center frequency of 2608 MHz. It is easily available for a reasonable price and has a small footprint. Its main disadvantages are that its bandwidth does not allow for the full 200 MHz transmit bandwidth and its ripple in the pass band.

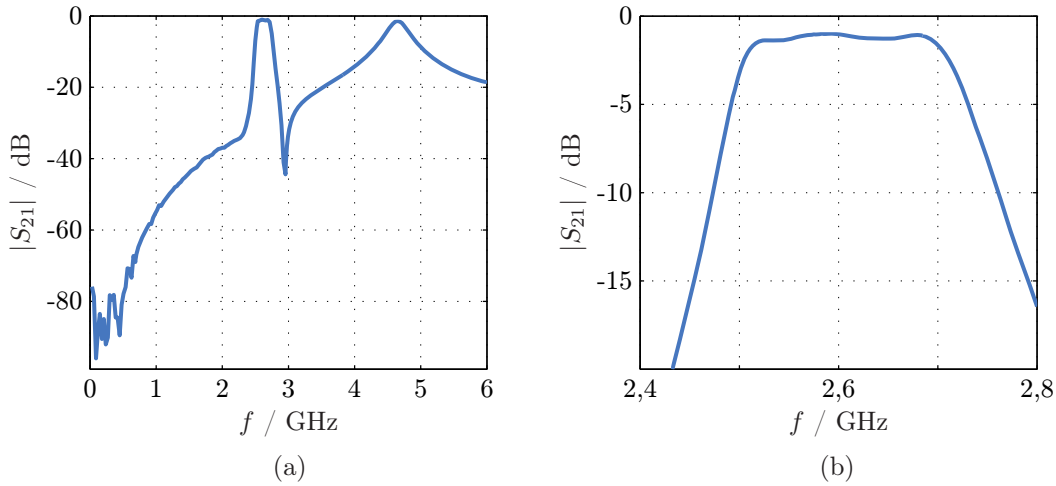

Figure 4.6: Frequency response of the NTK MFE2593CCF21 filter.

Both the bandwidth and the ripple can be increased and decreased respectively by replacing the filter by another custom made filter. This allows for a higher pole count and for a flexible positioning of the poles. Such filters can be easily designed with software from different manufacturers (see [8] or [9]). On the other hand such filters have long lead time and high setup costs.

One could also combine a lowpass and a highpass filter to form a broad bandpass filter. Such a combination of off-the-shelf filters has been tested. It resulted in a higher insertion loss and – relatively speaking – hough bandwidth. As can be seen in Figure 4.6(a) the chosen filter from NTK has a second pass band near the 3rd harmonic of the local oscillator LO2. The combination of lowpass and highpass filter does not have a second pass band in this spectral region. It therefore can be considered as a good alternative.

4.5 Buffer Amplifier

Before the RF signal carries on through the next parts of the "RF2600" section its level is increased. As buffer amplifier I chose a MGA61563 from Agilent [10]. It has a gain of 16 dB in the desired frequency range. Its 1 dB compression point $P_{1\text{dB}}$ and 3rd order intercept point IP_3 are at 16 dBm and 32 dBm output power

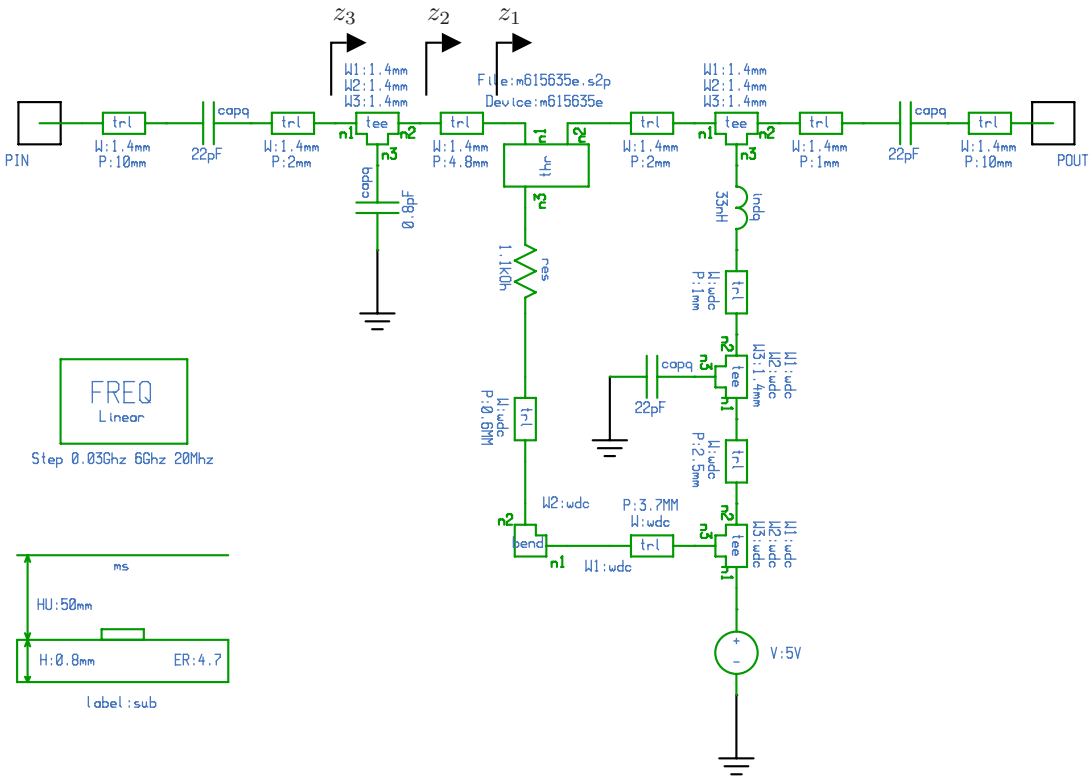

Figure 4.7: Schematic of the buffer amplifier.

respectively. To reach these values it needs a good input matching network. The schematic of this network is shown in Figure 4.7 on the left side. Figure 4.8 shows the corresponding Smith Chart (see [1] ch. 3.4, [4] ch. 2.2).

The complex input impedance Z_1 of the buffer amplifier is $25{,}5 + 2{,}6j\ \Omega$ at 2,9 GHz. The position for this impedance is marked in Figure 4.7. The corresponding reflection coefficient ϱ_1 is calculated using

$$\varrho = \frac{Z/Z_0 - 1}{Z/Z_0 + 1} = \frac{z - 1}{z + 1}\ , \tag{4.6}$$

where z is the normalized complex impedance related to the characteristic impedance of the system $Z_0 = 50\,\Omega$. This reflection coefficient is the starting point for the matching network. It is also marked with the label z_1 in the Smith Chart shown in Figure 4.8. A microstrip line with $50\,\Omega$ is added. This corresponds to walking on a circle with constant magnitude of the reflection coefficient (ϱ=const) in the Smith Chart in clockwise direction. After 31,2° electrical length we reach the circle where the normalized conductance equals 1 (g=1). This is marked with z_2. The physical length of such a microstrip line is 4,8 mm on the PCB substrate used as can be seen in the schematic. A shunt capacitor is added with a value of 0,8 pF. Such a capacitor corresponds to walking on a circle with constant conductance, changing only the susceptance. The matching point with $\varrho = 0$ is

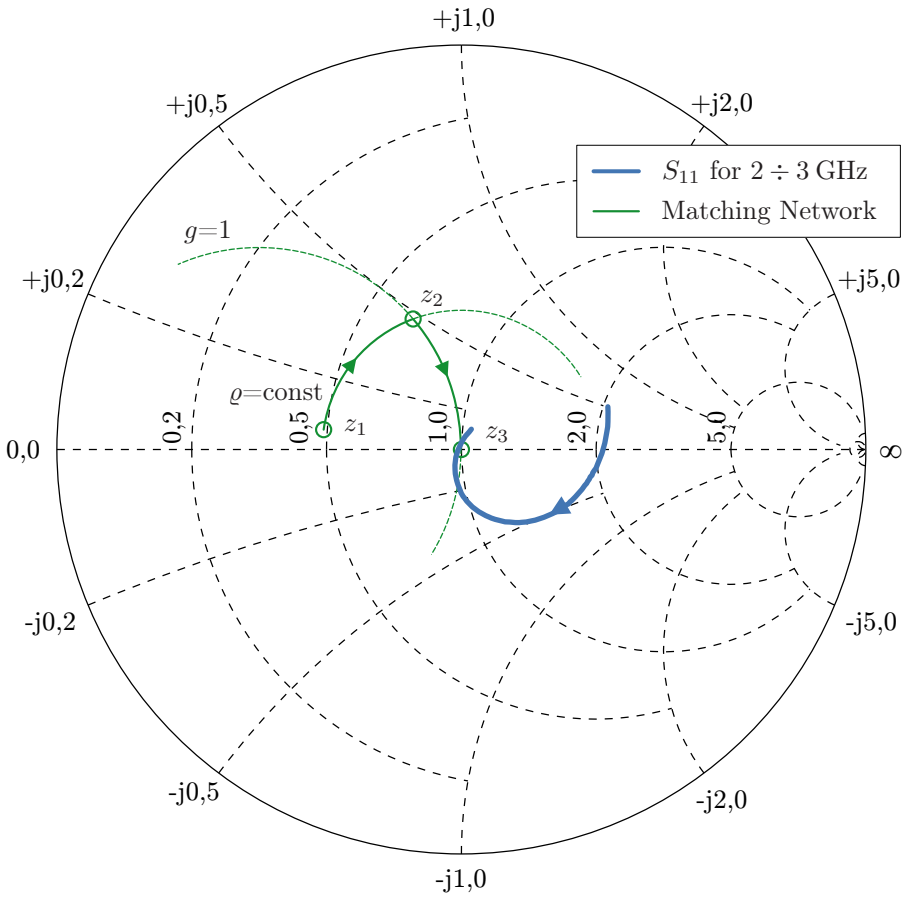

Figure 4.8: Smith Chart of the input matching network for the buffer amplifier.

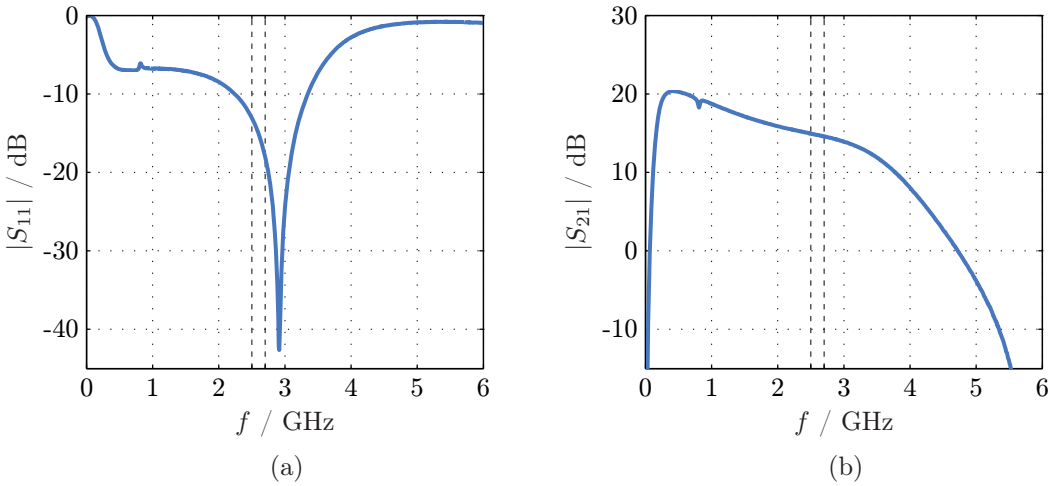

Figure 4.9: Input match and gain of the buffer amplifier.

reached (label z_3 in the figures) for this frequency. The resulting S_{11} is shown in Figure 4.9(a).

At the output the buffer amplifier is already properly matched. It only needs a simple biasing circuit. This is shown in Figure 4.7 on the right side. It consists of a resistor to set the bias current and an RF choke combined with a shunt capacitor. At 5 V supply voltage the bias current chosen is 50 mA.

Last but not least I placed DC blocking capacitors at the input and output. This is to decouple the DC bias voltage from the preceding and following circuits.

The buffer amplifier is used in a frequency range from 2500 to 2700 MHz. However the matching network described above is designed for 2900 MHz. One major problem with the amplifier chosen is its declining gain with increasing frequency. This can be compensated for by shifting the resonance frequency of the matching network. This is the reason why the matching network has not been designed for 2600 MHz. An optimum shift was chosen between maximal flatness of the frequency response and best matching. The result is shown in Figure 4.9(b). It is clearly visible that the slope is less declined in the region of interest than in the remaining range.

4.6 Switch

The "RF2600" section has two RF outputs. The HMC232 from Hittite [11] allows to switch one input to one of two outputs. Those are the transmitter mode output described in Section 4.7 and the test mode output described in Section 4.8. The key parameters of the device are given in Table 4.2.

Table 4.2: Specification of the switch.

Parameter	Value	Unit
Frequency range	0 ÷ 8	GHz
Negative supply voltage	-5	V
Positive supply voltage	0	V
Insertion loss	1,3	dB
Isolation	51	dB
Return loss	17	dB

As external components it only needs a DC driver and level shifter circuit. This circuit is based on a logic device (74HC04) augmented with a zener diode, a resistor, and some blocking capacitors and is shown in Figure 4.10(a) at the bottom. The resulting layout for the test PCB is shown in Figure 4.10(b). The inputs and outputs are labeled with the signal names as used in the "RF2600" section.

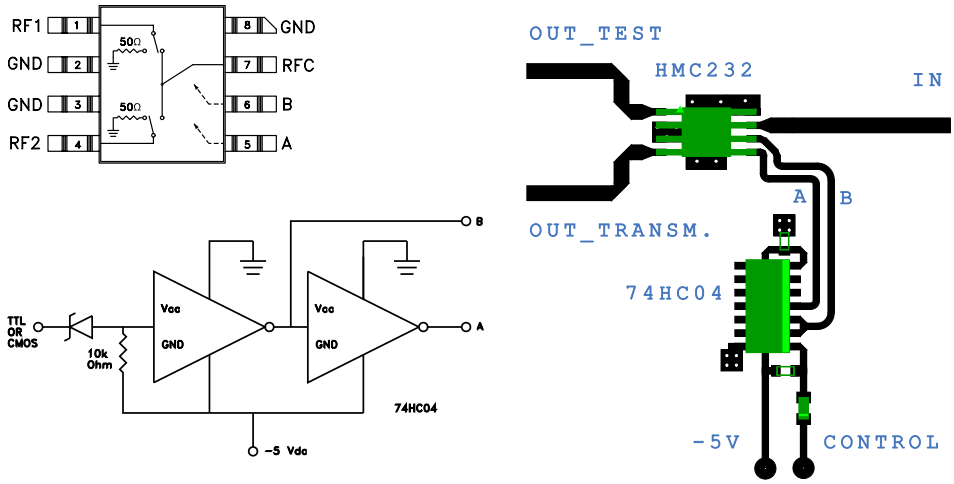

(a) (b)

Figure 4.10: Schematic [11] and layout with part outlines of the RF switch.

4.7 Transmitter Mode Output

After the switch one branch leads to the transmitter mode output. It delivers +13 dBm power at a 50 Ω SMA connector and can be directly connected to an accordingly matched antenna. Figure 4.11 gives an overview. Its specification has already been given in Section 4.2 and Table 4.1.

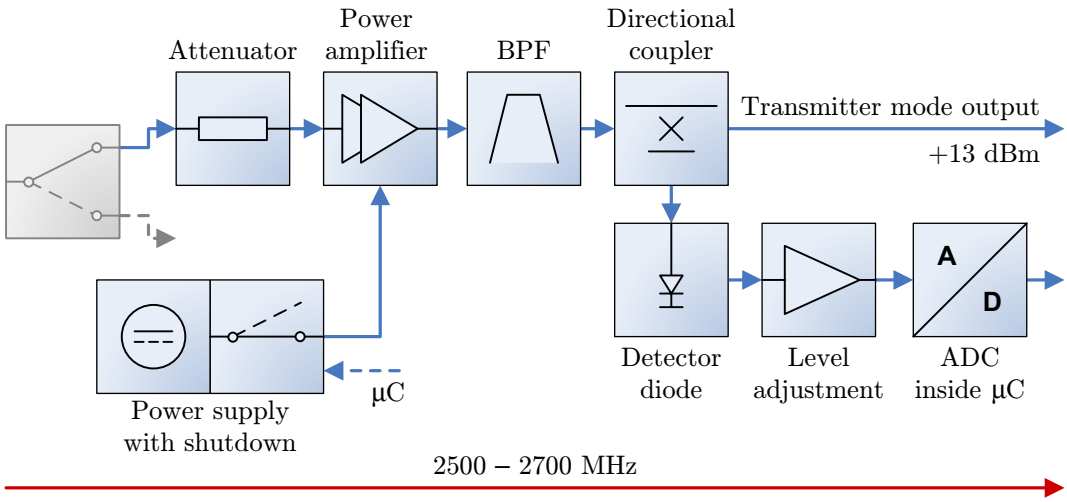

Figure 4.11: Overview of the transmitter mode output branch.

The transmitter mode output consists of a power amplifier with a trailing bandpass filter. The filter is again a NTK MFE2593CCF21 as earlier described in Section 4.4. At last there is a directional coupler which allows to draw out a fraction of the signal and measure its power level. This is described in sections 4.7.2

and 4.7.3. Measurement of the power level allows for feedback to the first transmitter section or the baseband hardware. The variable attenuators can then regulate the output power.

In front of the power amplifier there is another Π-style attenuator. It has a similar purpose as the one before the mixer and is normally short circuited with a 0 Ω resistor. If the transmitter mode output is not needed at all it does not have to be equipped with components. The attenuator is then used with a 50 Ω shunt resistor to terminate the switch.

4.7.1 Power Amplifier

As power amplifier I chose the MGA83563 from Agilent [12]. It needs only a single supply voltage of +3 to +3,3 V. A low drop voltage stabilizer is used to reduce the supply voltage from +5 V. It has a built in shutdown option which can be used to turn off the power amplifier. This is useful if the transmitter is in standby mode or the test mode output is used. The voltage regulator and shutdown switch can be seen in Figure 4.11.

The MGA83563 is a two stage amplifier. Its key figures are given in Table 4.3.

Table 4.3: Specification of the power amplifier.

Parameter	Value	Unit
Frequency range	0,5 ÷ 6,0	GHz
Supply voltage	3,0 ÷ 3,3	V
Small signal gain	22,0	dB
Saturation output power	+22,0	dBm
Output power at 1 dB compression point	+19,2	dBm

Since it does not need a matching network at input or output, it is easily set up. Only a inductor is needed to complete the impedance match between the first and the second stage. It is not current-biased but voltage-biased, so connecting the supply voltage in series with an RF choke to the amplifier is sufficient.

The most critical design step with setting up this power amplifier is the correct decoupling of the two stages and buffering of the supply voltage. Several different capacitors where needed to eliminate potential oscillation.

4.7.2 Directional Coupler

The directional coupler has a coupling factor[4] of 6,5 dB and a directivity of 23 dB. It is a bidirectional coupler called BDCA1-7-33 from Mini-Circuits [13]. As a consequence the backwards coupling branch has to be terminated with a 50 Ω

[4] see [1] ch. 8.1

resistor. The forward output can be terminated with a resistor too to deactivate the power sensor. However, normally it delivers a proportional signal with maximal +8 dBm for the transmitter output branch to the power sensor.

4.7.3 Power Detector

The power detector delivers the feedback signal to the micro controller. This is used to control the output power via the variable attenuators located on the first transmitter section. It is neither a peak power detector nor a true averaging sensor. It is rather a short term averaging sensor.

Detector Diode

As detector diode I chose an HSMS286K from Agilent [14]. It is a small outline (SOT363) Schottky detector diode optimized for the use from 915 MHz to 5,8 GHz. Two well isolated diodes with similar parameters are located in the same housing.

The diode can either be used directly (i.e. zero bias) or with DC bias. Two diodes can be combined with a differential amplifier for better temperature compensation. Here this approach together with biasing has been taken.

Biasing and Differential Amplifier

The bias current for the diodes is set using a reference voltage and a series resistor. According to [15] the current should be chosen in the range from 3 μA to 30 μA for maximal output voltage. To get better tolerance from the input current of the subsequent differential amplifier I chose a slightly larger value of 42 μA.

A resistive input matching network has been used. For the diode in the reference path of course no matching network is needed. The influence of this difference was neglected.

The differential amplifier is built up using the easily available operational amplifier TLV272 from Texas Instruments and a feedback network with resistors. It serves as a differential amplifier as well as a subtraction circuit of a small offset voltage. This offset is necessary to reach suitable output ranges. In this first amplification stage only a small gain of 1,67 is set.

Level Adjustment

After the first differential amplifier a second operational amplifier of the type TLV272 is used to set the final output range. It does not have to add a further voltage shift, nor does it have to take any offset current problems into account. For the transmitter output branch the cumulative gain of first and second amplifier is set to 2,8.

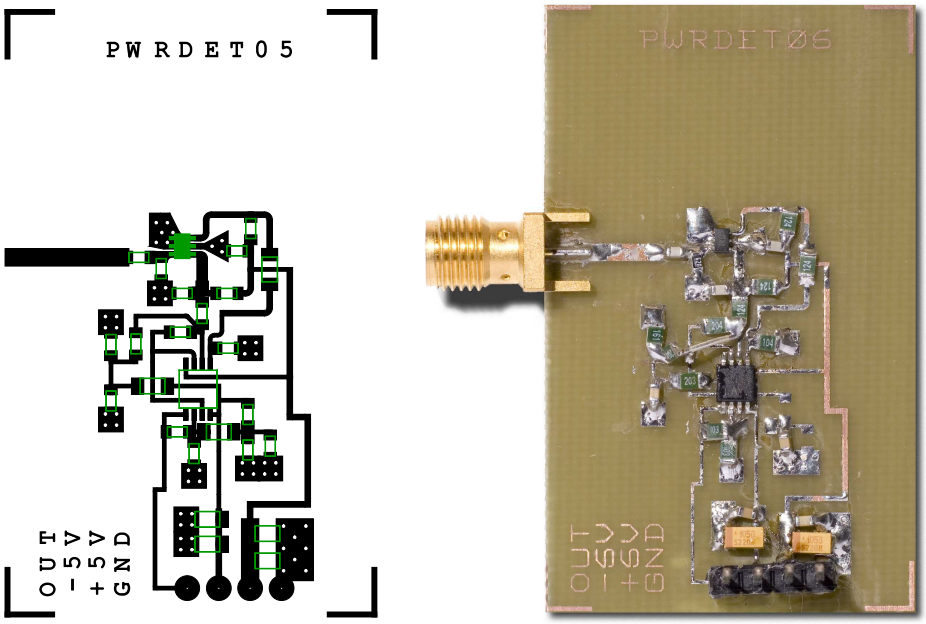

(a) (b)

Figure 4.12: Layout and assembled test PCB of the power detector.

At its output the power detector circuit delivers a voltage from 0 to 3 V to the ADC located inside the micro controller. The maximum input power of +8 dBm results in a output voltage near 3 V. The correlation between input power and output voltage is not optimized to be logarithmic or corresponding to the square law of the diode. However it is monotonous. The micro controller has to take care of the correct translation from measured voltage to interpreted power level (e.g. by means of a lookup table).

All described components where first combined onto a test PCB. The resulting layout is shown in Figure 4.12(a). Figure 4.12(b) shows the final PCB where measurements have been taken.

Figure 4.13(a) gives the relation between input power and output voltage of the complete power detector for the transmitter mode path and the test mode path which will be described in Section 4.8.3. Since the power shall be measured on a logarithmic scale Figure 4.13(b) illustrates the same relation as Figure 4.13(a) in a logarithmic way. An offset voltage of $U_{off} = 0{,}09$ V has been compensated for in this figure. The ripple in the low power range of the plot for the transmitter mode output is due to the coarse resolution of the measurement equipment during this measurement.

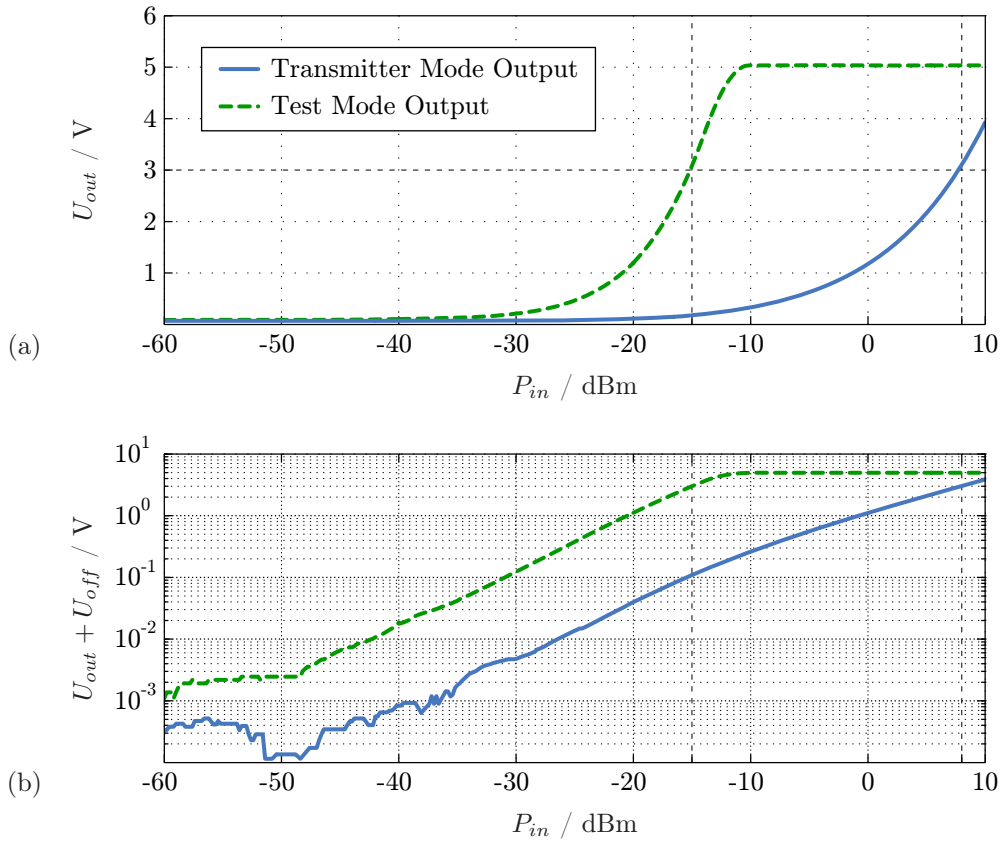

Figure 4.13: Output voltage as a function of input power for the power detector.

4.8 Test Mode Output

Beside the transmitter mode output there is the test mode branch. Its purpose is to allow for a direct connection to a receiver or an external power amplifier stage. Figure 4.14 gives an overview of this branch. In contrast to the transmitter mode output you cannot see a level adaption attenuator nor another amplifier. Instead it allows for variable attenuation described in Section 4.8.2.

4.8.1 Specification

Table 4.4 gives the detailed power level plan for the test mode output. It starts with the output of the switch which is directly taken from Table 4.1. The goal of this branch is to achieve −10 dBm maximum power at its output and to allow for further variation of the level.

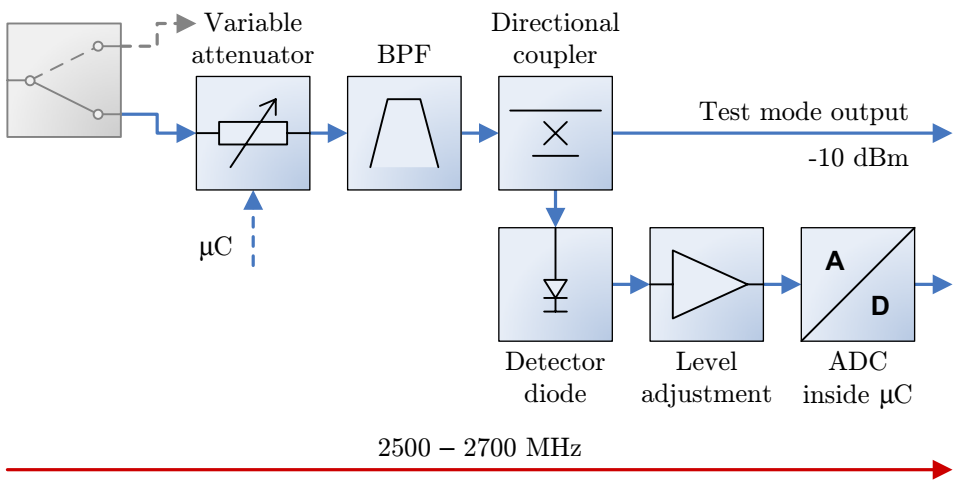

Figure 4.14: Overview of the test mode output branch.

Table 4.4: Power level plan for the test mode branch of the "RF2600" section.

Component	f_c MHz	G dB	F dB	P dBm	F_{total} dB
Input from switch	2600			-4,5	14,5
Variable attenuator	2600	-2,5	2,5	-7,0	14,6
Bandpass filter	2600	-1,0	1,0	-8,0	14,6
Directional coupler	2600	-2,0	2,0	-10,0	14,6
Output test mode	2600			-10,0	

4.8.2 Variable Attenuator

Instead of a fixed attenuator the test mode branch has got a variable attenuator. It is a HMC 346 from Hittite [16]. This is the same device as used on the 1 GHz section of the transmitter. It gives you the possibility of 30 dB attenuation.

For external components it needs an high speed operational amplifier used in a regulation loop. With this circuit it can convert a control voltage of 0 to −3 V into an attenuation of 0 to 30 dB. The resulting schematic is shown in Figure 4.15. Again a test PCB was built up as illustrated in Figure 4.16.

Table 4.4 only gives the parasitic attenuation of this device. If attenuation is switched off the desired output power of −10 dBm for this output path can be achieved.

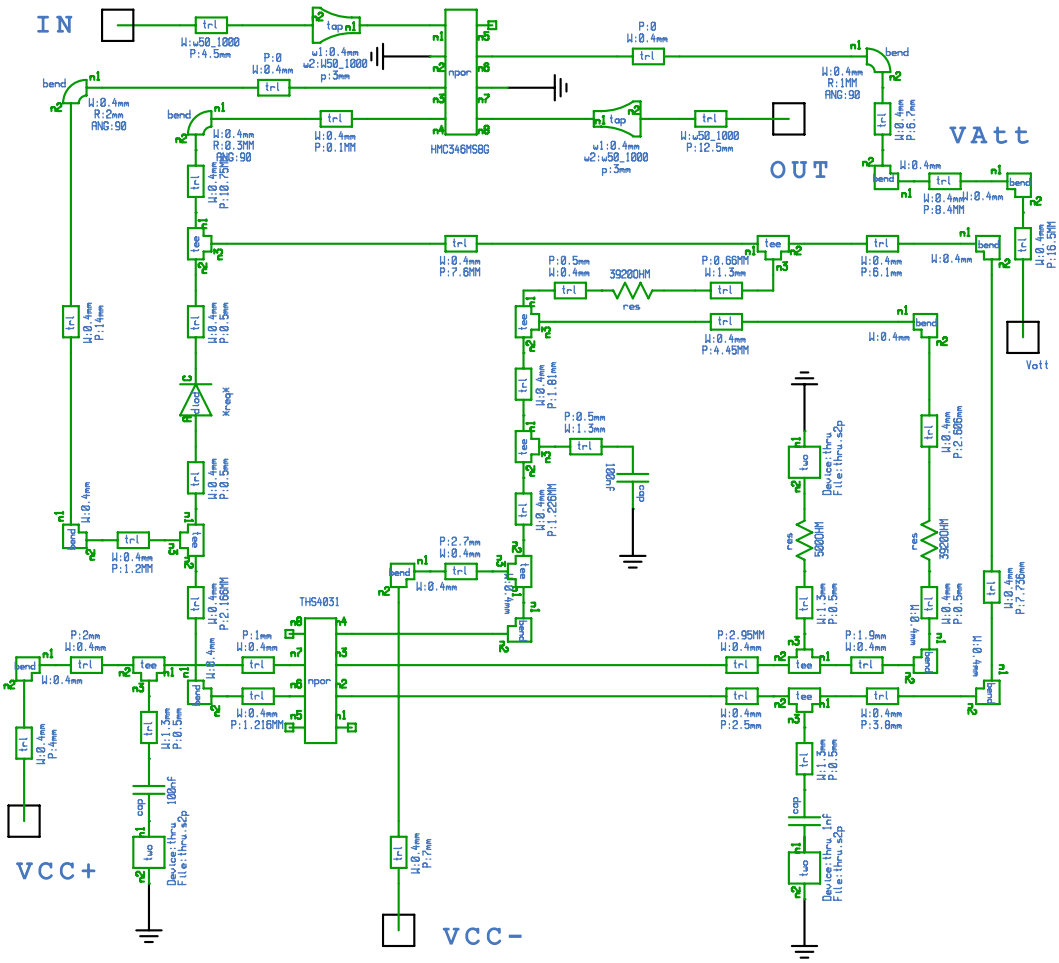

Figure 4.15: Schematic of the variable attenuator.

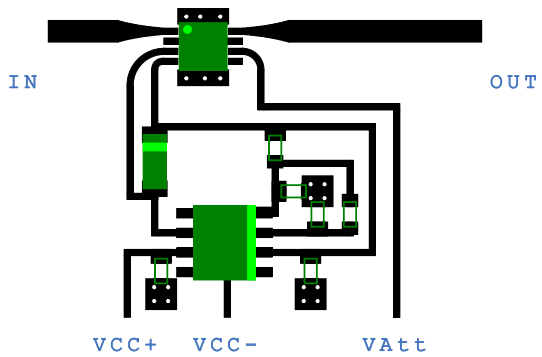

Figure 4.16: Layout and part outlines of the variable attenuator.

4.8.3 Power Detector

As can be seen in Figure 4.14 after the variable attenuator there are another bandpass filter, directional coupler and power detector. These blocks are almost identical to those in the transmitter mode output branch and have already been described in sections 4.7.2 and 4.7.3.

The power detector of course needs to be adjusted for the different power range. This is accomplished by different values of the offset voltage in the first stage and the gain in the second amplifier stage. The gain of the level adjustment amplifier is set to 44. This means that a maximum input power to the power detector of -15 dBm is converted to an output voltage of slightly less then 3 V. The exact value is uncritical since its interpretation is again left to the micro controller and a lookup table. Figures 4.13(a) and 4.13(b) again show the measurement results of the complete power detector without the micro controller.

4.9 “RF2600” Section PCB

All components described so far were combined on a single PCB. This is then mounted atop the base PCB as described in Section 3.2. Several modification where necessary compared to the test PCBs described in the previous sections. They affected the routing and stabilizing of the DC power supply.

Figure 4.17 shows the final layout of the “RF2600” section PCB. Special care has been taken on the positions of the SMA connectors. The positions determine the routing of the semi rigid cables to the front panel of the transmitter. When the “RF2600” section is redesigned for a different output frequency band, a change of all those cables is not required. Figure 4.18 shows the final assembled PCB which measured parameters are given in the next chapter.

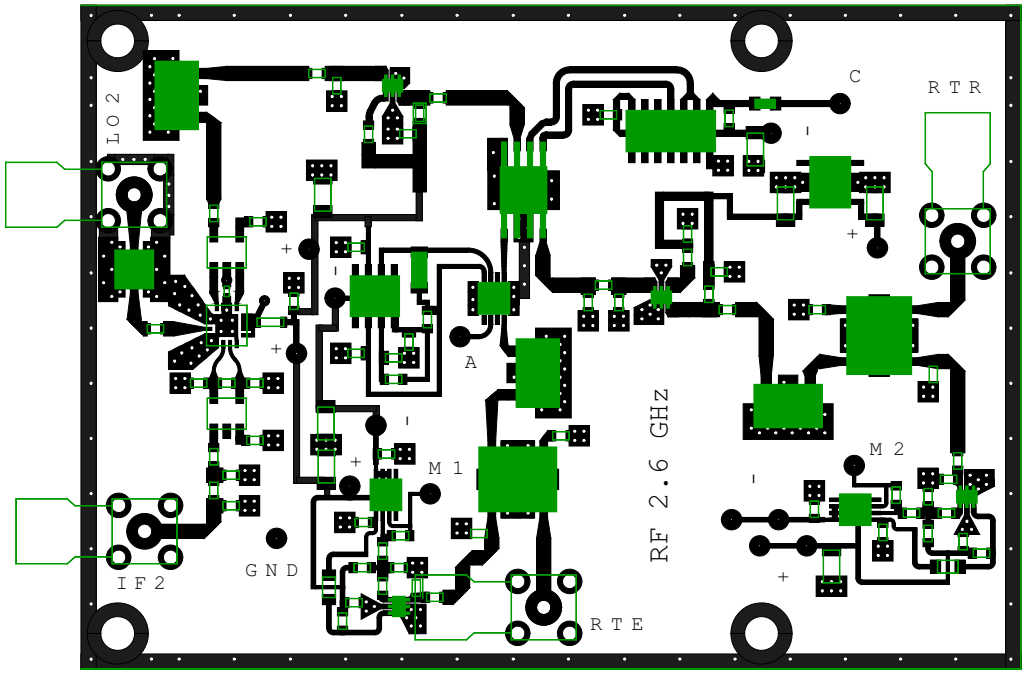

Figure 4.17: Complete layout and part outlines of the “RF2600” section.

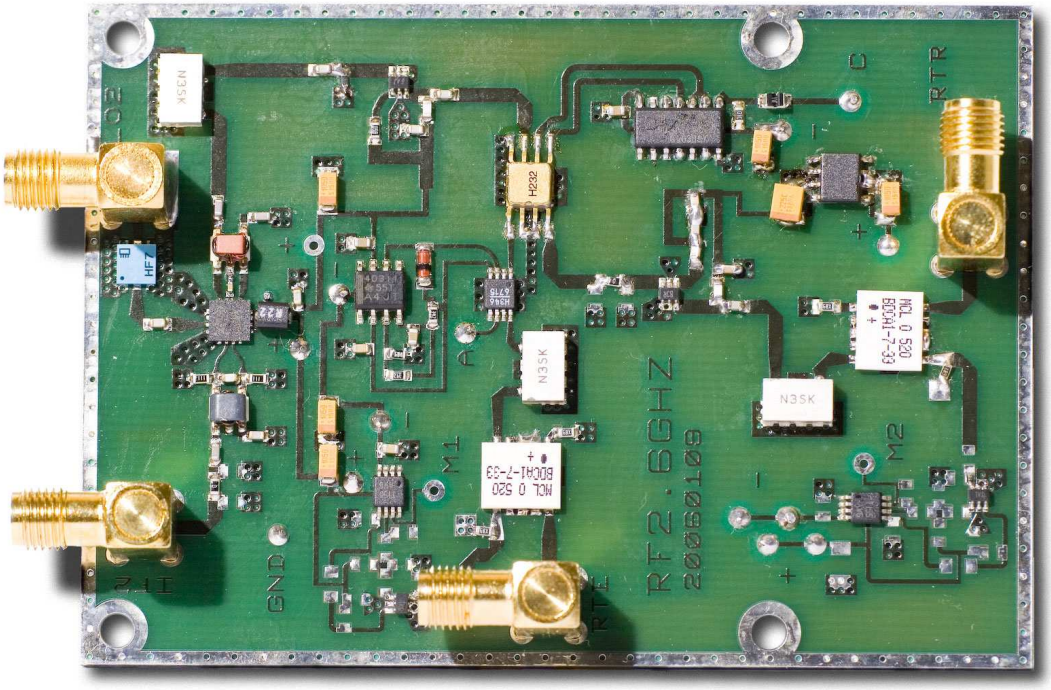

Figure 4.18: Photo of the “RF2600” section PCB.

Chapter 5

Performance Measurements

The transmitter – as described in Chapter 3 – consists of two analogue parts. The second upconversion stage – the "RF2600" section described in Chapter 4 – has been characterized by measurements which will be presented in this chapter. Further, several measurements have been performed on the complete transmitter, which will also be presented here.

Measurements have been taken using a vector network analyzer, a vector spectrum analyzer, and different signal sources. All of these instruments have a GPIB[1] connector or a similar interface by means of LAN[2]. Using these interfaces they can be remotely controlled from any PC. Matlab [17] has been used as a high level programming language to send the correct commands to the instruments and read out the measurement results.

5.1 Frequency Response

The frequency responses of the "RF2600" section and the complete transmitter have been measured using a 4-port VNA[3] as shown in Figure 5.1. It has two individual signal sources, so one can be used as the input signal and the other one as the second local oscillator. An external signal generator has to be used as the first local oscillator input for measurements on the complete transmitter. It is remote controlled by the VNA using GPIB. Figure 5.2 shows this setup. The DUT shown is the RF transmitter unit equipped with four complete transmitter cards.

Figure 5.3 shows the frequency response of the "RF2600" section PCB. The second local oscillator LO2 is fixed at $f_{\mathrm{LO2}} = 1652{,}5\,\mathrm{MHz}$ while the input signal is swept. Both – input and output – frequencies are given on the horizontal axis. The frequency range shown is extremely large since the maximally allowed input bandwidth is specified with 40 MHz. Consequently the slope in the upper range is no problem. The transmitter mode output has a gain of 26,4 dB while the test mode output has a gain of 5,9 dB.

[1] General Purpose Interface Bus (IEEE 488)
[2] Local Area Network
[3] Vector Network Analyzer

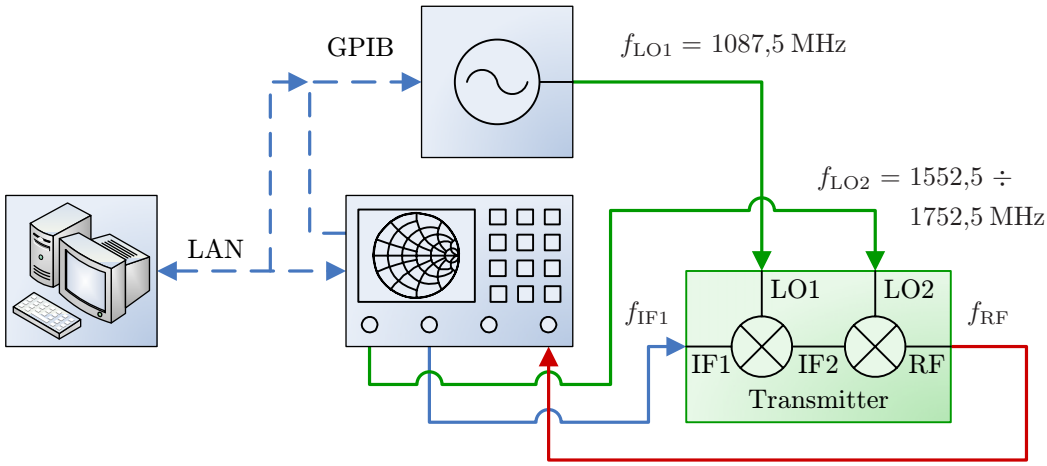

Figure 5.1: Block diagram of the setup for measuring the frequency response of the complete transmitter.

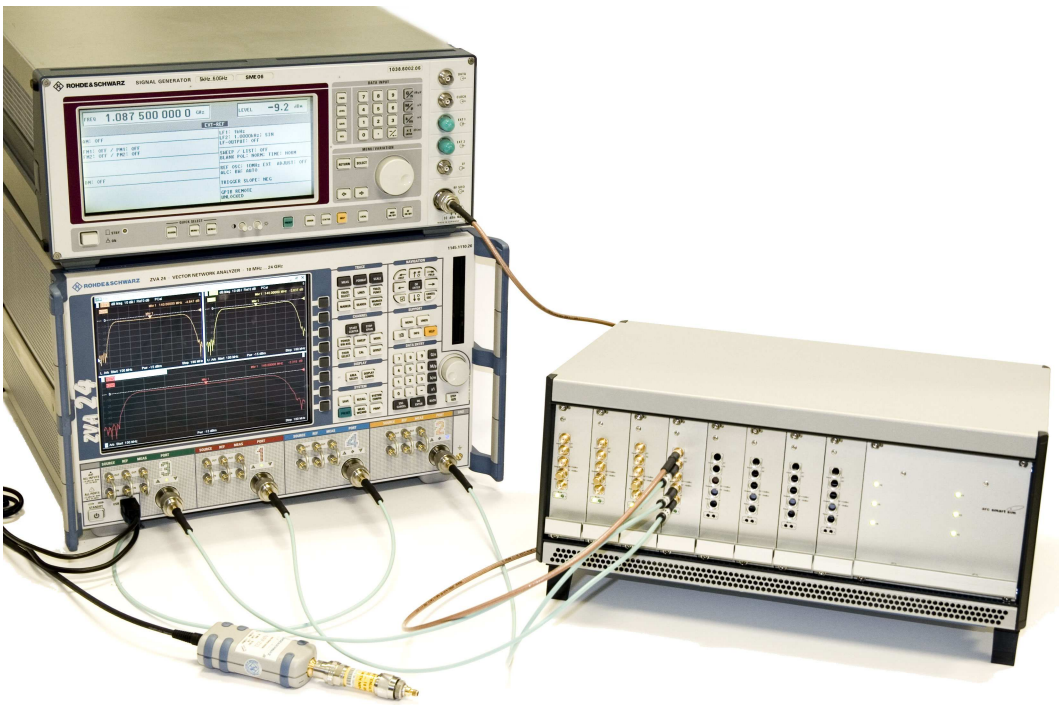

Figure 5.2: Photo of the setup used for measuring the complete transmitter.

The gain is a function of the chosen output center frequency by means of the second local oscillator. This is shown in Figure 5.4 for the test mode output. Again both frequencies are given on the horizontal axis. This time the input signal at IF2 is fixed while the local oscillator LO2 is swept. The measured range extends the specified range of 200 MHz to show the degradation at the edges of the output band. The variation of the gain is mostly the direct result of the used transmit filter (also see Figure 4.6(b)).

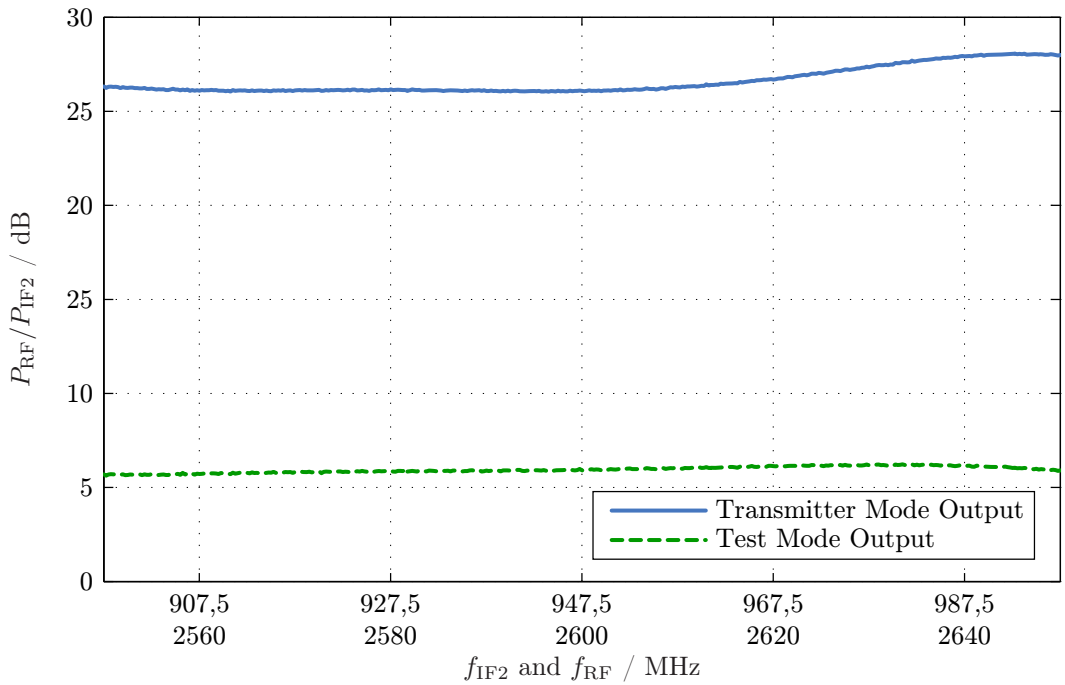

Figure 5.3: Frequency response of the "RF2600" section as a function of the input frequency f_{IF2}.
$P_{IF2} = -15\,\text{dBm}$, $f_{LO2} = 1652{,}5\,\text{MHz}$, $P_{LO2} = -3\,\text{dBm}$

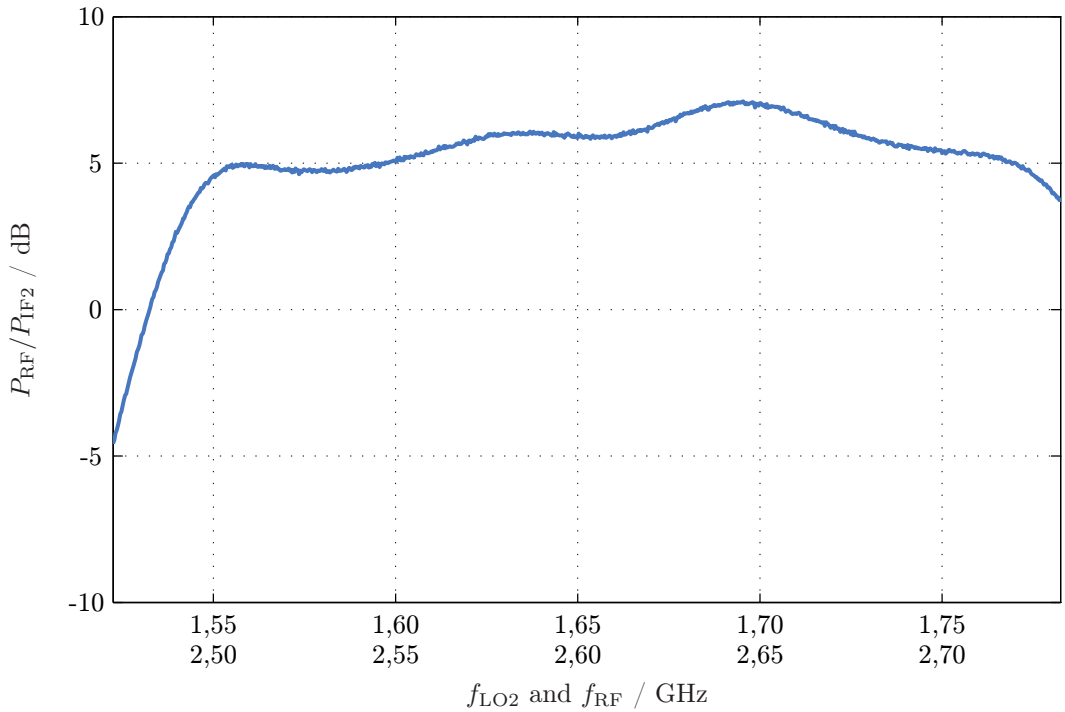

Figure 5.4: Frequency response of the "RF2600" section as a function of the second local oscillator frequency f_{LO2} for the test mode output.
$f_{IF2} = 947{,}5\,\text{MHz}$, $P_{IF2} = -15\,\text{dBm}$, $P_{LO2} = -3\,\text{dBm}$

While figures 5.3 and 5.4 show the frequency response of only the "RF2600" section, Figure 5.5 shows the response of the complete transmitter. The plot in the middle corresponds to the settings used for Figure 5.3. The other plots show the frequency response for different settings of the second local oscillator LO2. The outer plots extend beyond the specified output frequency range. The frequency range has been split into eleven adjoining bands with 20 MHz bandwidth. The second local oscillator has been adjusted for each of these center frequencies and measurements have been taken. The measurements have been concatenated accordingly and the result is shown in Figure 5.6. The dashed lines in the outer regions show the measurements at the edges of the transmit band.

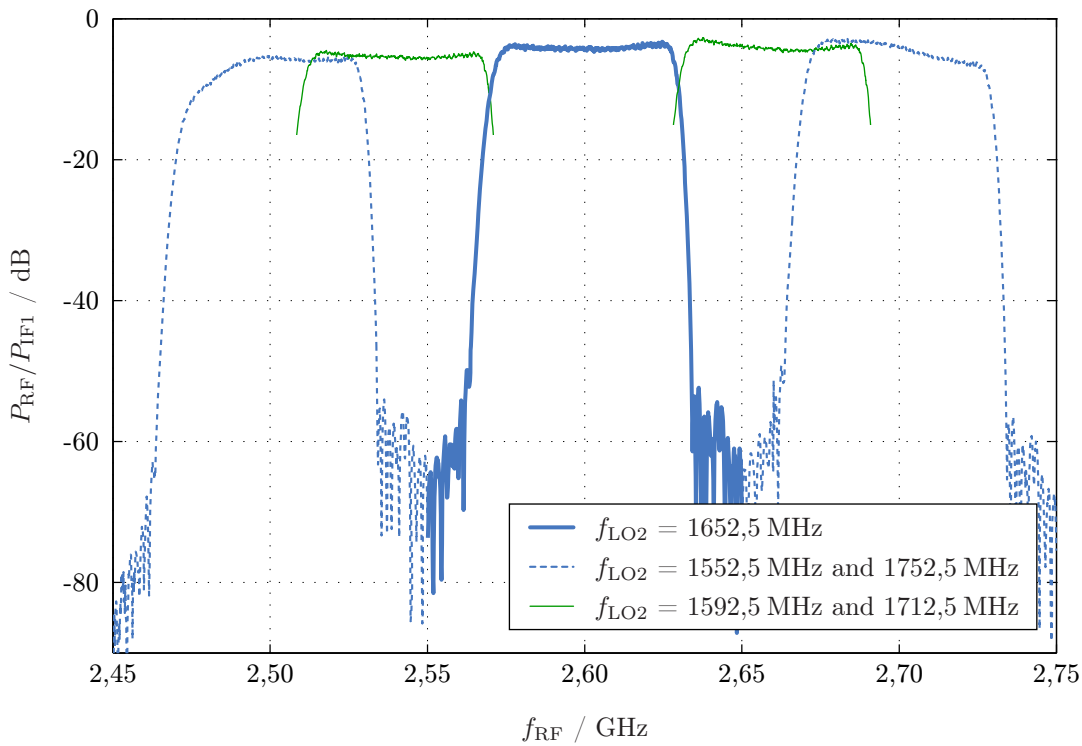

Figure 5.5: Frequency response of the complete transmitter.

Since the frequency response is dependant on both – input frequency and output frequency – I also examined the impact of the bandwidth of the input signal. The minimal and maximal conversion gain for various input bandwidths has been measured and is plotted as a function of output center frequency in Figure 5.7. Table 5.1 gives the results for the higher bandwidths. The second column f_{RF} gives the actually measured output frequency range and does not correspond to the input bandwidth. The measurement for 50 MHz bandwidth already exceeds the specified input frequency bandwidth. For the maximally allowed bandwidth of 40 MHz the mean conversion loss of the complete transmitter is 4,3 dB. It has a maximal variation of 2,2 dB although the typical variation is as low as 1,0 dB.

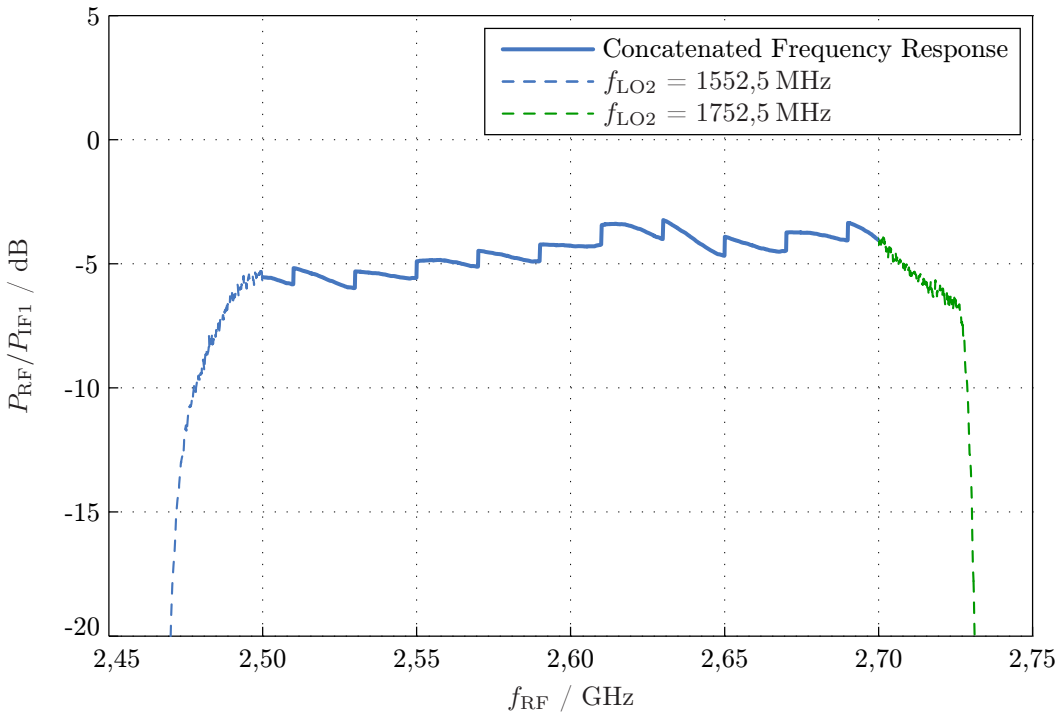

Figure 5.6: Full concatenated frequency response of the complete transmitter.

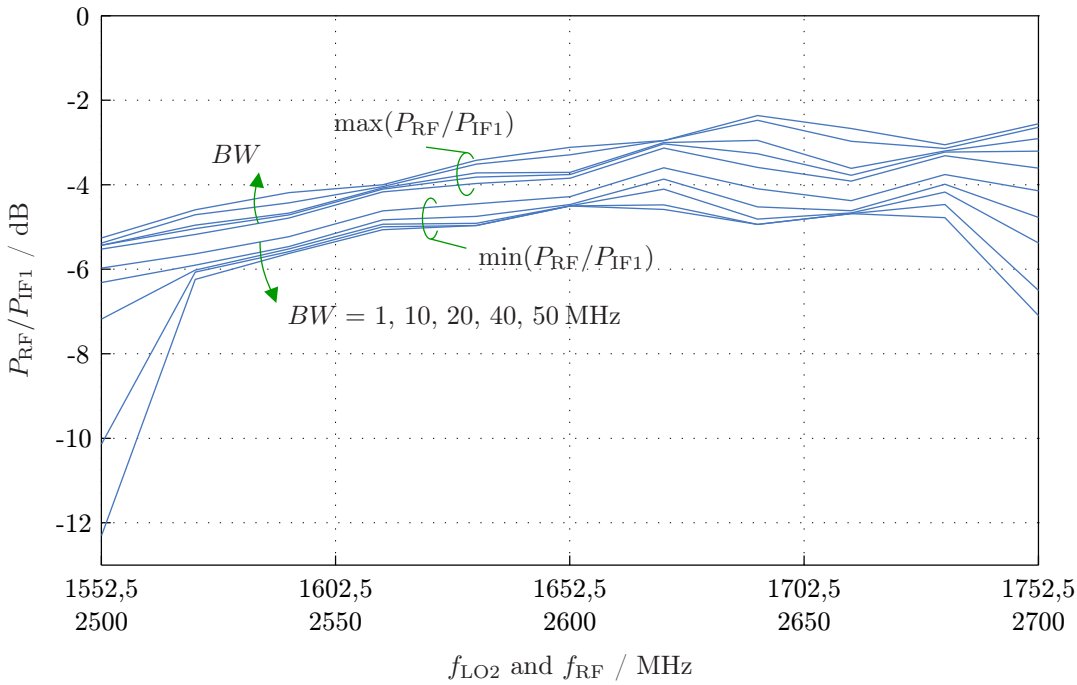

Figure 5.7: Variation of the conversion gain of the complete transmitter as a function of the LO2 frequency and the IF1 bandwidth.

Table 5.1: Conversion gain and its variation at various LO2 frequencies f_{LO2} and measurement bandwidths BW for the complete transmitter.

	$BW =$	20 MHz		40 MHz		50 MHz	
f_{LO2} MHz	f_{RF} MHz	G dB	ΔG dB	G dB	ΔG dB	G dB	ΔG dB
1552,5	2450-2550	-6,0	1,5	-6,5	4,5	-6,8	6,8
1572,5	2470-2570	-5,5	0,7	-5,4	1,0	-5,4	1,2
1592,5	2490-2590	-5,1	0,5	-5,0	0,7	-5,0	1,0
1612,5	2510-2610	-4,5	0,5	-4,5	0,5	-4,5	0,7
1632,5	2530-2630	-4,3	0,8	-4,3	1,0	-4,2	1,1
1652,5	2550-2650	-4,1	0,4	-4,0	0,8	-3,9	1,0
1672,5	2570-2670	-3,5	0,8	-3,6	1,1	-3,7	1,2
1692,5	2590-2690	-3,9	1,5	-3,8	2,0	-3,8	2,1
1712,5	2610-2710	-4,2	0,6	-4,0	1,3	-3,9	1,6
1732,5	2630-2730	-3,7	0,6	-3,7	1,0	-3,8	1,3
1752,5	2650-2750	-4,0	2,2	-4,2	3,5	-4,2	4,1

5.2 Output Power and Power Compression

The transmitter has two outputs. Figure 5.8 shows the output power of the transmitter mode output as a function of the power P_{IF2} into the "RF2600" section. The specified nominal input power to this section is -12 dBm. For this power level the output power of $+13$ dBm is reached. However the output power is not increasing linearly with the input power any more. For too high input power the output power saturates and reaches the maximal value of $P_{sat} = 16{,}7$ dBm.

Figure 5.9 shows the gain for transmitter and test mode output. Initially the gain for the transmitter mode output is 26,4 dB as already given in Section 5.1. As the input and output power reach -12 dBm and $+13$ dBm respectively the gain degrades. At -13 dBm input power it has dropped by 1 dB which is called the 1 dB-compression point. The output power is 12,4 dBm then (P_{1dB} in Figure 5.8).

For the test mode output the 1 dB-compression point is not reached until 4,5 dBm input power. This is well above the nominal input power and stands for the better performance of this RF path.

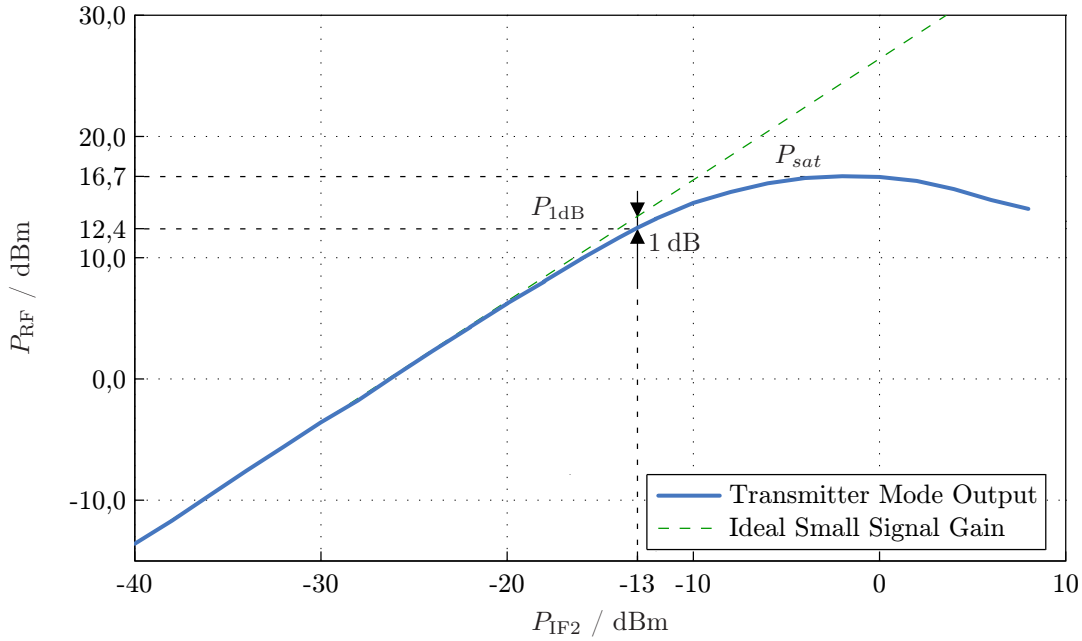

Figure 5.8: Output power as a function of input power for the "RF2600" section PCB measured at the transmitter mode output.
$f_{\mathrm{IF2}} = 947{,}5\,\mathrm{MHz}$, $f_{\mathrm{LO2}} = 1652{,}5\,\mathrm{MHz}$, $P_{\mathrm{LO2}} = -3\,\mathrm{dBm}$

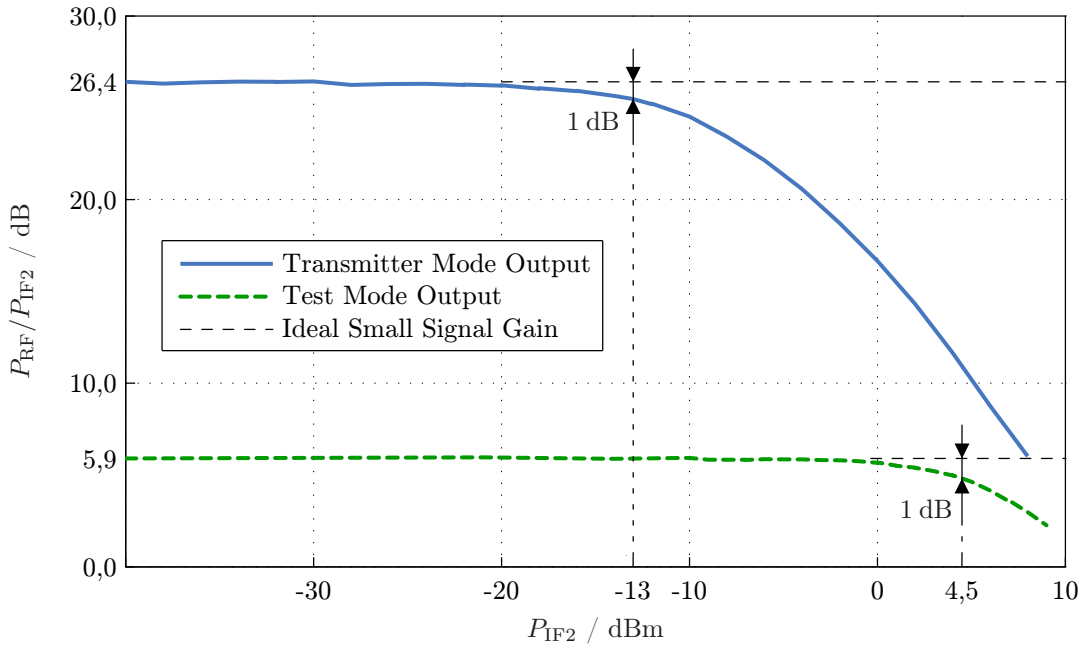

Figure 5.9: Gain of the "RF2600" section PCB as a function of input power.
$f_{\mathrm{IF2}} = 947{,}5\,\mathrm{MHz}$, $f_{\mathrm{LO2}} = 1652{,}5\,\mathrm{MHz}$, $P_{\mathrm{LO2}} = -3\,\mathrm{dBm}$

5.3 Intermodulation

Intermodulation is the result of nonlinearities in the DUT and its components (see [5] ch. 9.2.3.2.2, [1] ch. 11.2). Here these are mainly the mixer, the buffer amplifier, and the power amplifiers. Traditionally intermodulation is measured using two-tone input signals like those shown in Figure 5.11(a). They can be generated using two signal generators and combining there outputs as depicted in Figure 5.10. Additional attenuators in front of the power combiner are used to decouple the two sources. The input frequencies f_{1i} and f_{2i} are chosen close to each other in a distance Δf. The measurements presented here use a value of $\Delta f = 1\,\text{MHz}$, although other values have been used too with similar results. At the output of the DUT a signal similar to Figure 5.11(b) is measured with a spectrum analyzer.

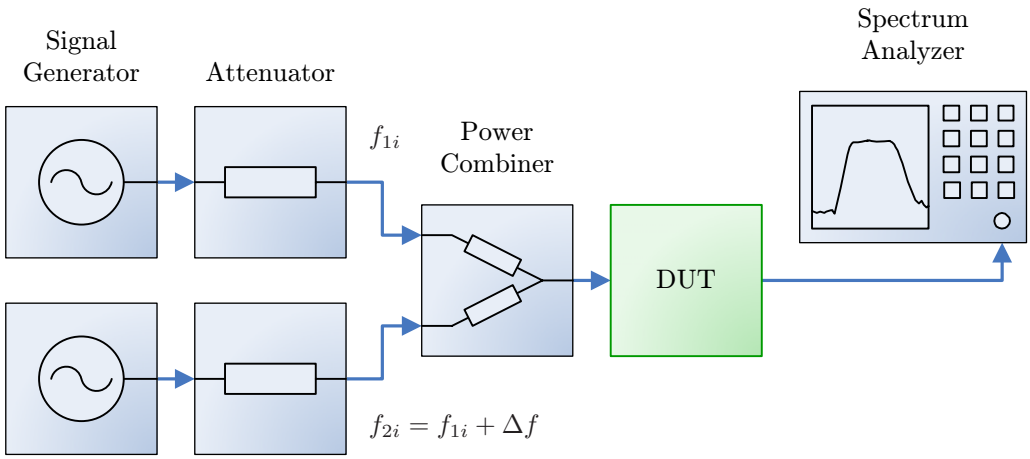

Figure 5.10: Traditional two-tone setup for intermodulation measurements.

Since our DUT – the "RF2600" section – is a frequency converting device, the output appears shifted to other frequencies, which are denoted by f_1 and f_2. At higher input powers new spectral components appear at $f_1 + f_2$, $f_1 - f_2$, $2f_1 - f_2$, and so on. The components due to the quadratic (i.e. even order) term of the nonlinearity are far off the output frequencies. The odd order components (i.e. third, fifth,... order) fall near the output band. Figure 5.11 shows the input and output spectrum of the "RF2600" section.

The power P_1, P_3, P_5,... of each of the components is measured and the sum is plotted as a function of total input power. This is shown in Figure 5.12 for the test mode output and in Figure 5.13 for the transmitter mode output. At lower input powers there are no detectable intermodulation products on the output. The jagged part of the plots below $-80\,\text{dBm}$ is due to the noise floor of the spectrum analyzer. It depends on the input attenuator setting. Since the attenuator has been stepped in response to the total input power this results in a stepped noise floor. At higher input power the output power of the fundamental as well as of the intermodulation products saturate. Consequently they have

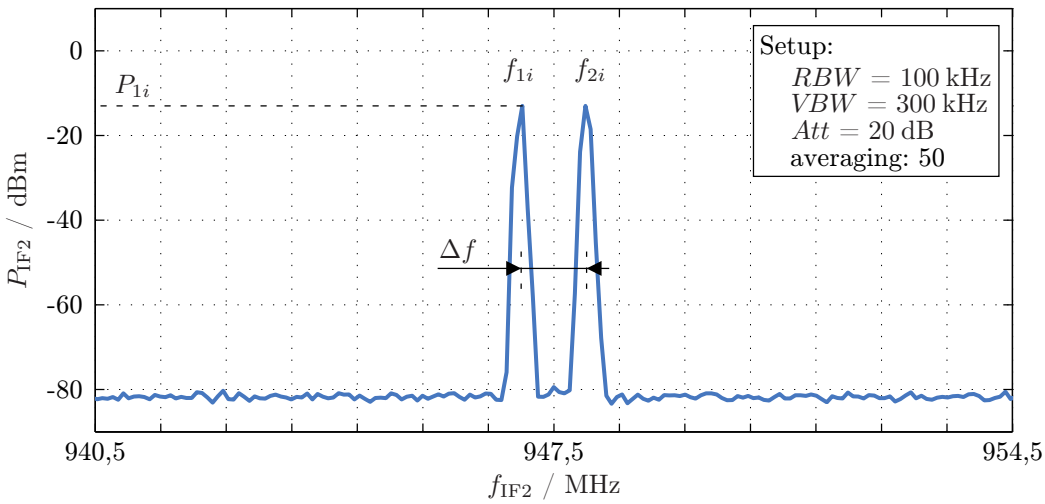

(a)

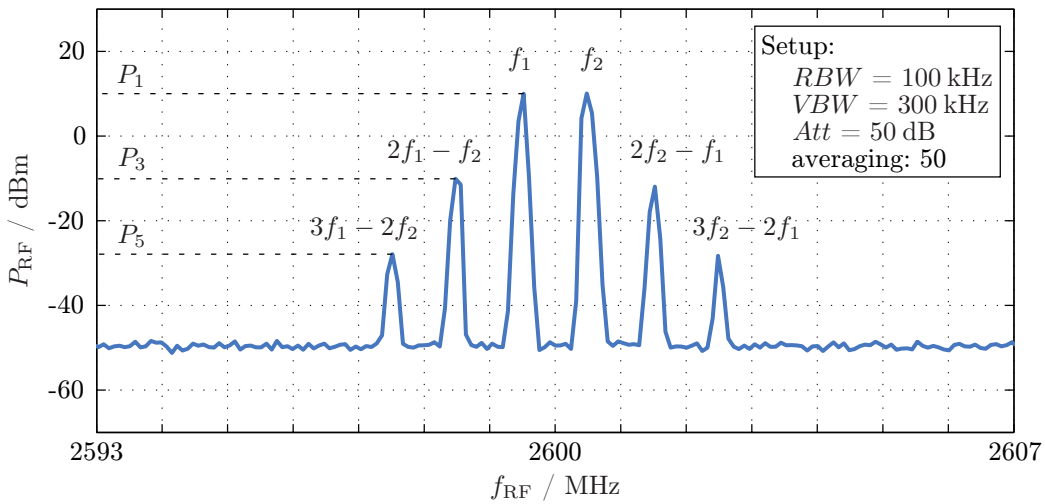

(b)

Figure 5.11: (a) Input and (b) output signals for the two-tone intermodulation measurement of the "RF2600" section.

been extrapolated linearly. The fictitious point where the total power of the intermodulation products of order x reaches the power of the fundamentals is called intercept point IP_x of order x. It can be given either by its output power value or its input power according to

$$IP_{x,in} \,/\, \mathrm{dBm} = IP_{x,out} \,/\, \mathrm{dBm} - G \,/\, \mathrm{dB} \ . \tag{5.1}$$

The results from these measurements are given in Table 5.2.

Besides the two-tone measurements, there are other ways to characterize the effects of nonlinearity of the transmitter. Real world signals from digital modulation formats typically occupy more bandwidth than $\Delta f = 1\,\mathrm{MHz}$. Using a 40 MHz wide noise source could be an option. However similar results can be

Table 5.2: Intercept points of 3rd and 5th order for the transmitter and test mode outputs.

	Input	Output	Unit
Test Mode IP_3	12,1	18,0	dBm
Test Mode IP_5	12,6	18,5	dBm
Transmitter Mode IP_3	-1,9	24,5	dBm
Transmitter Mode IP_5	-2,9	23,5	dBm

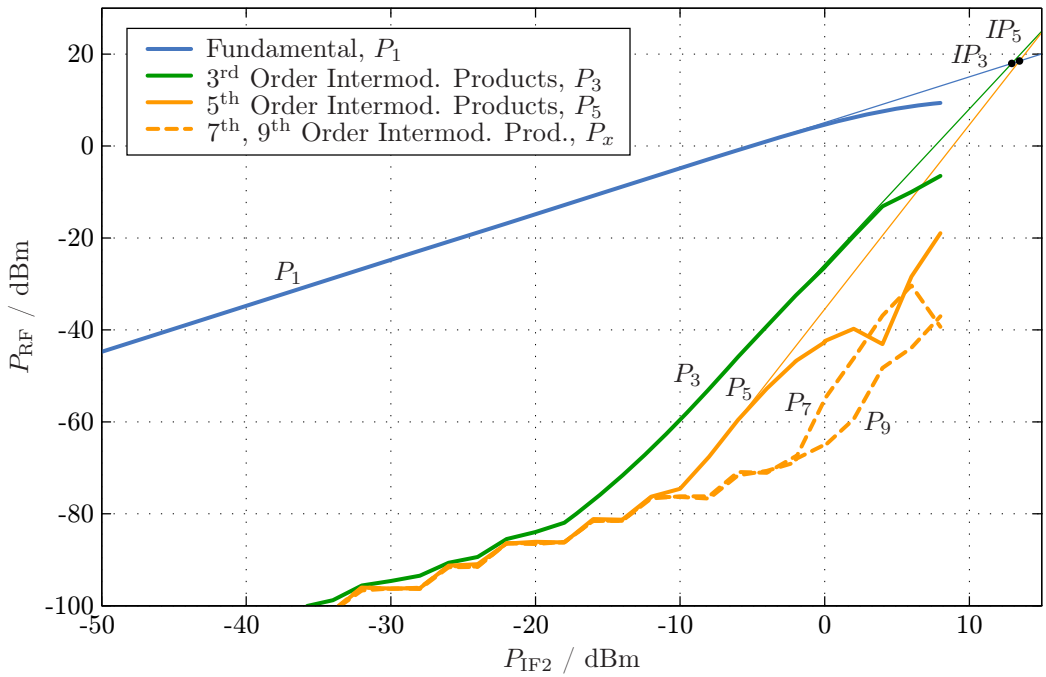

Figure 5.12: Power of the intermodulation products for the test mode output of the "RF2600" section.

achieved using multisine excitation. Such signals differ in count of sinewaves and their amplitude, frequency spacing, and relative phase. Good results can be obtained using more then ten beats with equal amplitude and spacing [18] [19]. Constant phase offsets lead to signals with hough crest factors CF, while random or Schroeder phase result in low crest factors [20] [21].

In these measurements I used a setup with an arbitrary vector signal generator[4] as depicted in Figure 5.14. The optimization of the phase was left to the signal

[4] R&S SMU200A

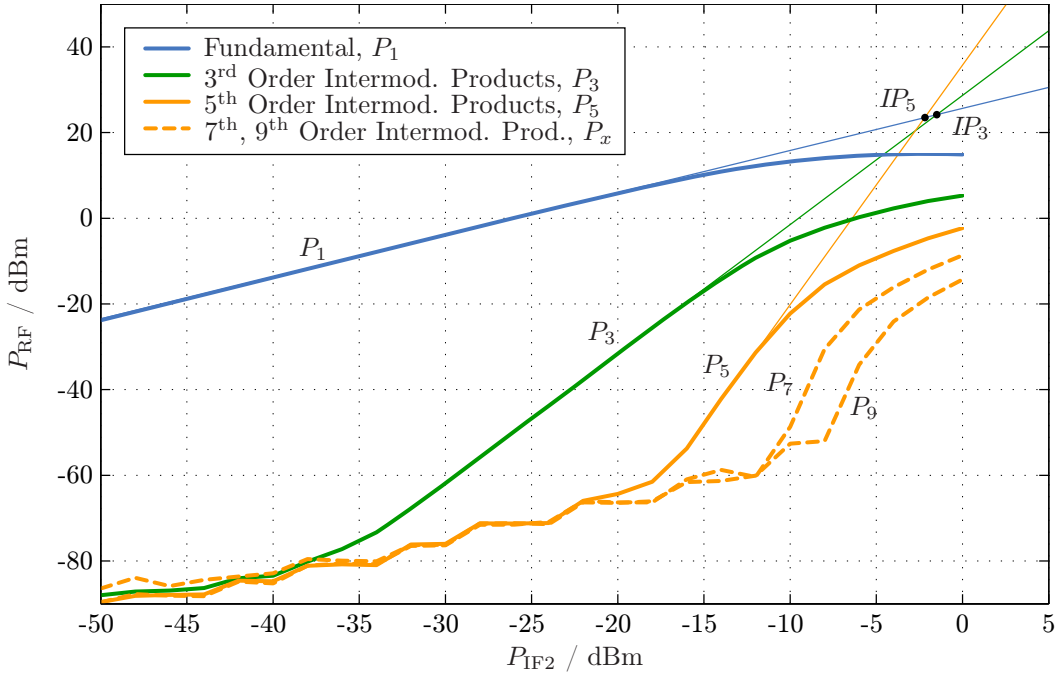

Figure 5.13: Power of the intermodulation products for the transmitter mode output of the "RF2600" section.

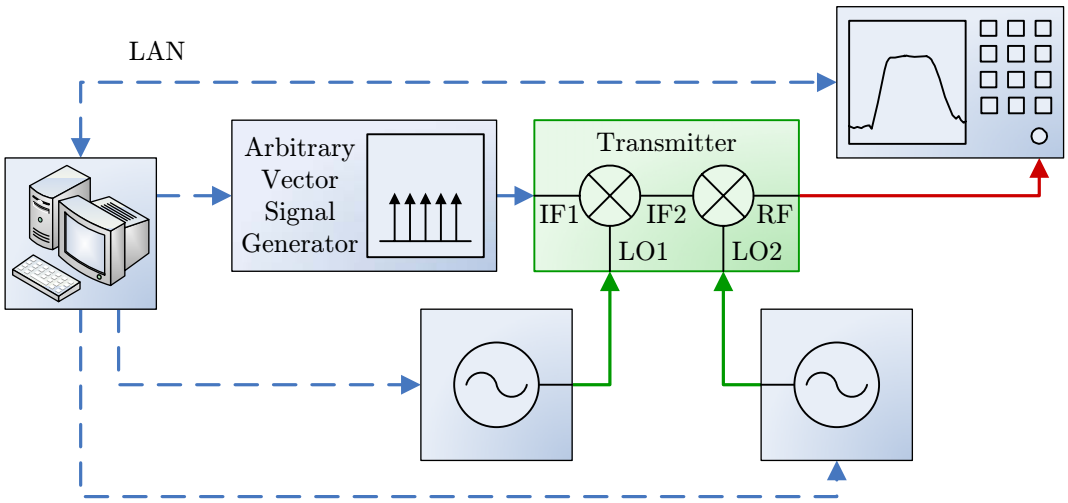

Figure 5.14: Versatile setup for measurements with double and multi beat signals.

generator. This resulted in even lower crest factors between 1,95 and 2,73 dB. Measurements were taken with 12 and 15 beats with 3,3 and 2,64 MHz spacing respectively, which results in an overall bandwidth of approximately 40 MHz. Since the spacing is constant all intermodulation products again fall on frequencies in this raster. They can affect the ranges below and beyond the desired output band

as well as there are in-band intermodulation products. The first is called adjacent channel distortion if it affects the the directly neighboring frequencies while the latter is called co-channel intermodulation. To measure in-band intermodulation, one of the beats has to be suppressed and the power is measured in this notch.

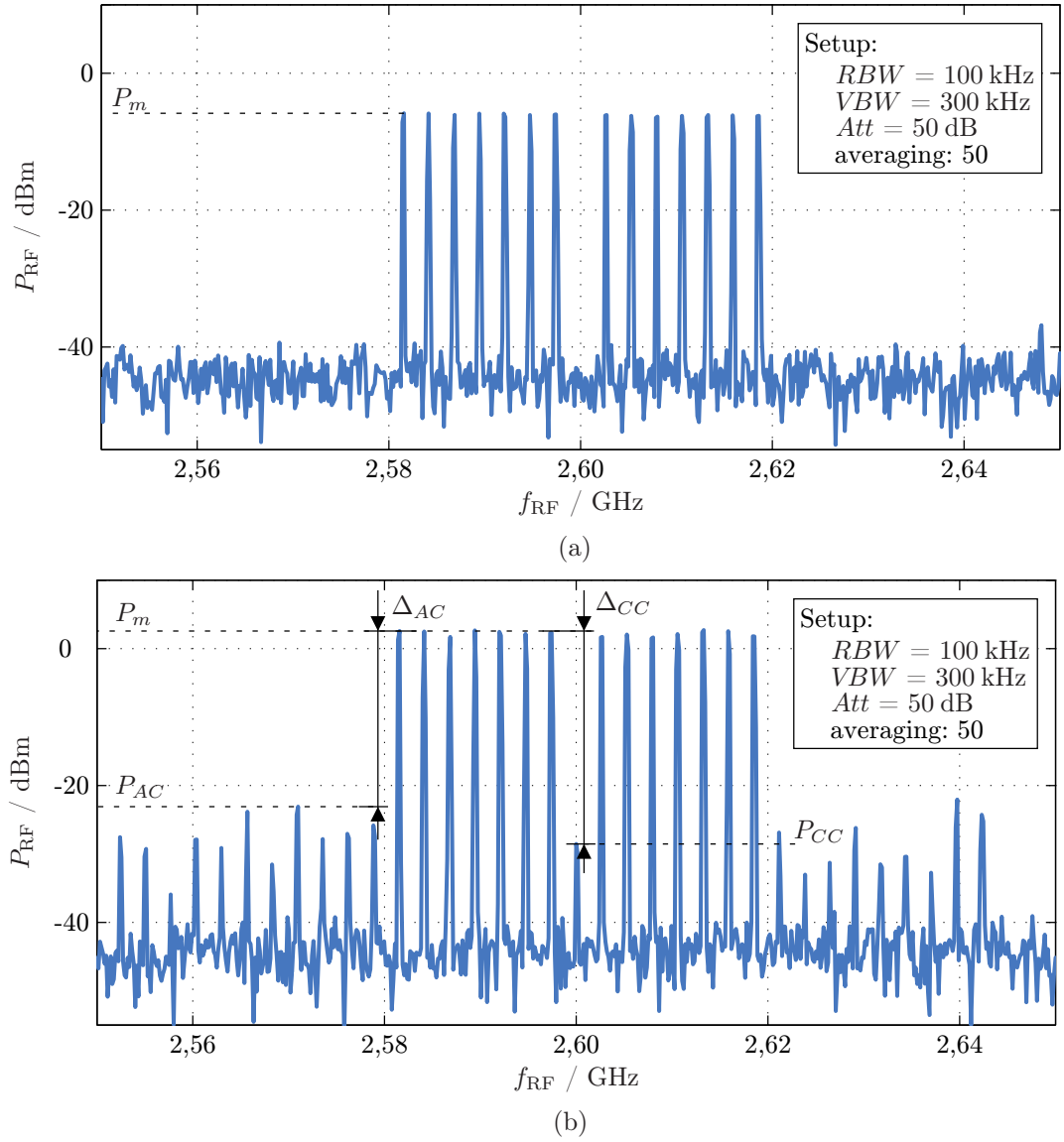

Figure 5.15: Spectrum of the multi beat signal at different input levels.

The output of the "RF2600" section for such a signal is shown in Figure 5.15(a). There are 15 carriers, the 8th is suppressed. The output power P_m of each of the carriers is measured and the total output power is summed up. At lower power levels this results in the RMS[5] input power enhanced by the gain of the transmitter section. As the input power increases, more and more intermodulation

[5] Root Mean Square

products arise in the adjacent channel as well as in the in-band notch as is shown in Figure 5.15(b). During each measurement the product with the highest power is detected and the ratio between this value and the total RMS power of the signal is determined. The resulting figures for this ratios – called *ACPR*[6] and *CCPR*[7] – are plotted as a function of total RMS input power in Figure 5.16. The *ACPR* can be used as a measure for the shoulder distance. At lower input powers – below −30 dBm for the transmitter mode output, below −10 dBm for the test mode output – the results are unreliable due to the noise floor of the spectrum analyzer.

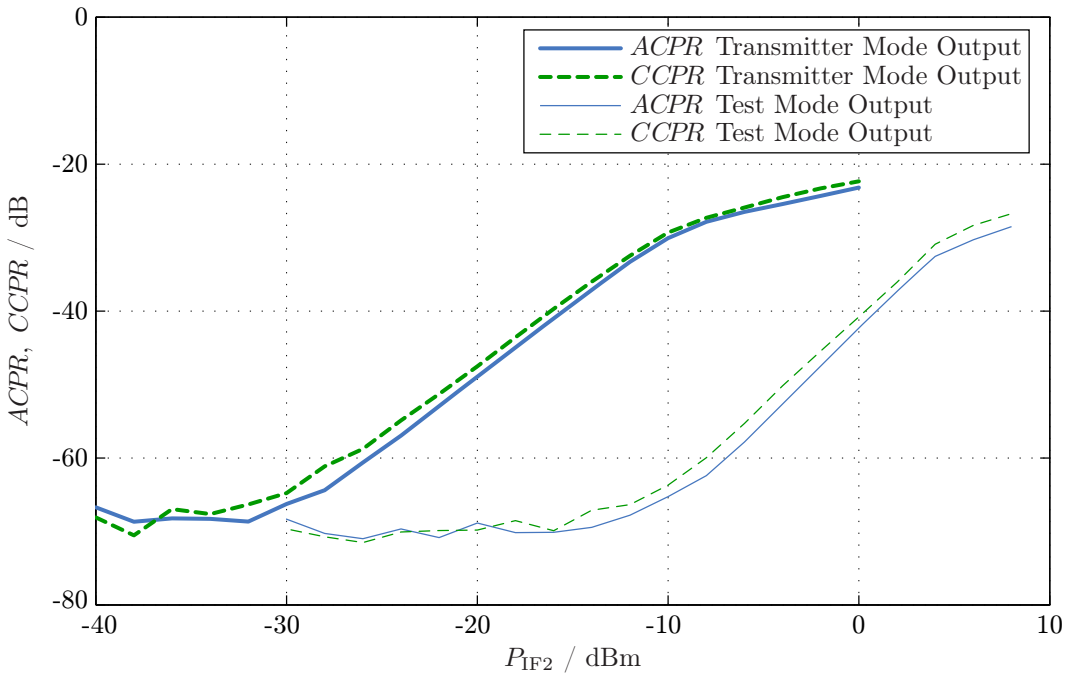

Figure 5.16: *ACPR* and *CCPR* as a function of the input power for the "RF2600" section.

5.4 Harmonics and LO Drive Power

As described in Section 4.3, after the mixing process there are not only the desired upper sideband but several other spectral components. Figure 5.17(a) shows the output of the transmitter mode path for various input signals. The lowest plot shows the noise floor of the spectrum analyzer and the measurement setup when the "RF2600" section is switched off. One can see that there is an interferer around 945 MHz[8] and the noise is not flat between 3 and 4 GHz.

[6] Adjacent Channel Power Ratio
[7] Co-Channel Power Ratio
[8] It is possibly the GSM-900 downlink which is located between 935 and 960 MHz.

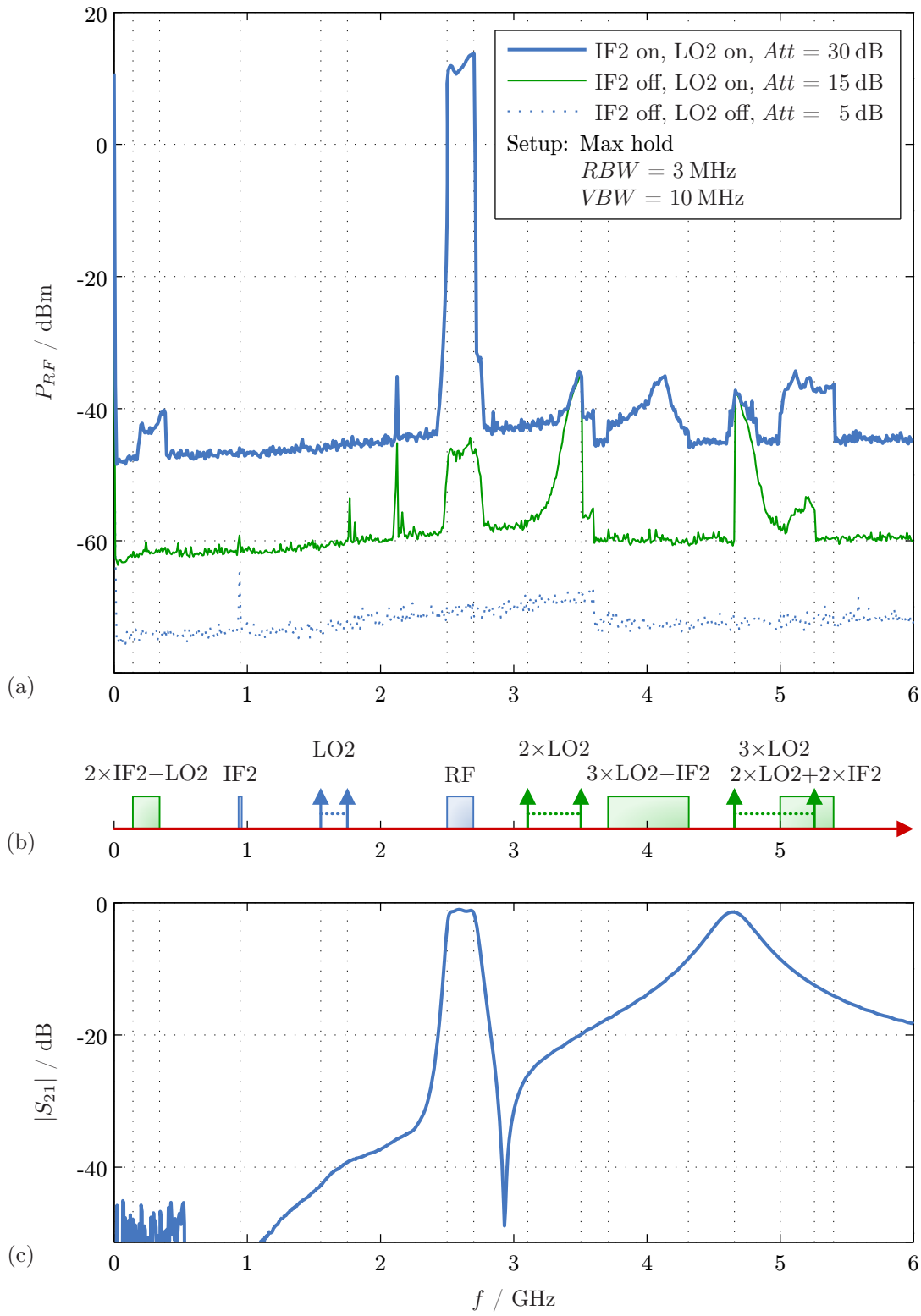

Figure 5.17: Overview of the output of the "RF2600" section. (a) Output spectrum at the transmitter mode output. (b) Spectral interpretation. (c) Frequency response of the transmit filter.

Next the "RF2600" section is switched on and the local oscillator LO2 is swept between 1552,5 and 1752,5 MHz. Since there is more power at the input of the spectrum analyzer now, the reference level and attenuator settings had to be adjusted. This results in a higher noise floor. At the output of the mixer there is the crosstalk of the harmonics of LO2. Second and third harmonics can be easily seen at the output. In Figure 5.17(b) an interpretation of Figure 5.17(a) is given. The positions of second and third harmonics are marked there as well as in the other two diagrams with vertical dotted lines. The shape of the harmonics reflects the shape of the transmit filter. Figure 5.17(c) therefore repeats the frequency response of the transmit filter already given in Figure 4.6(b) for comparison.

For the top plot of Figure 5.17(a) a monotone signal at 947,5 MHz is switched on as the input IF2 to the "RF2600" section. Now the remaining spectral components which are illustrated in Figure 5.17(b) become visible.

The 3rd harmonic of the local oscillator is the strongest undesired component at the output of the mixer which varies with the input power P_{LO2} of the local oscillator. It falls directly into the second passband of the transmit filter. The power of this component was measured as a function of LO2 input power and plotted in Figure 5.18 for the worst frequency setting. The use of $P_{\mathrm{LO2}} = -3\,\mathrm{dBm}$ is hereby verified.

Figure 5.19 gives the correlation between power of the local oscillator and the conversion gain. There is almost no variation at different power levels.

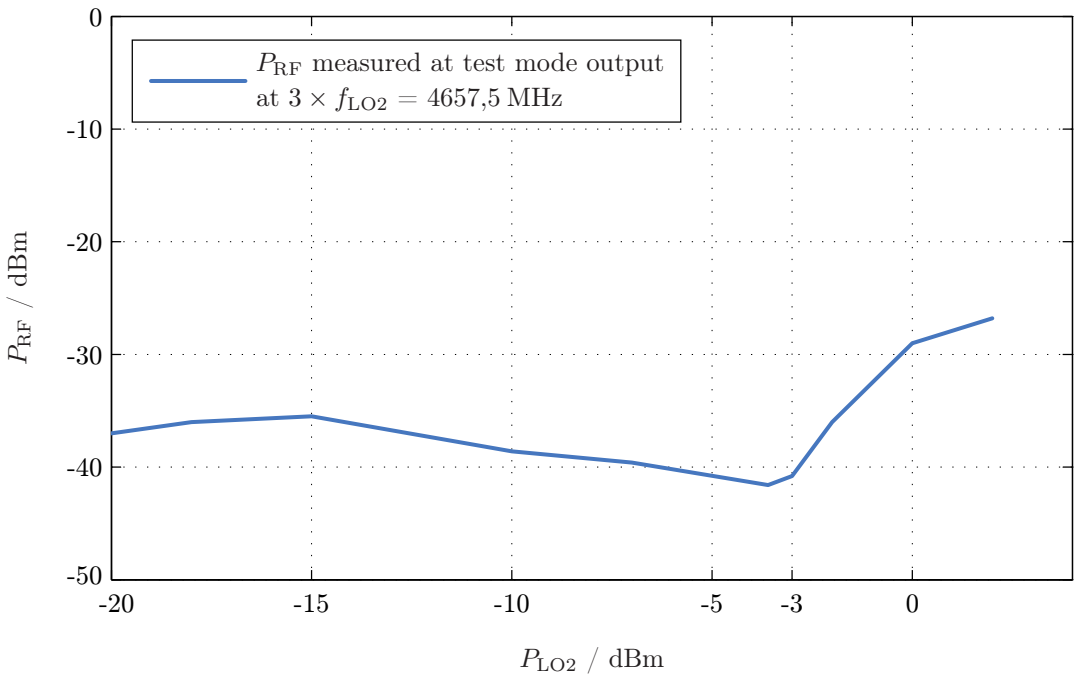

Figure 5.18: Power of the 3rd harmonics of LO2 at the test mode output as a function of the LO2 input power. IF2 is switched off, $f_{\mathrm{LO2}} = 1552{,}5$ MHz

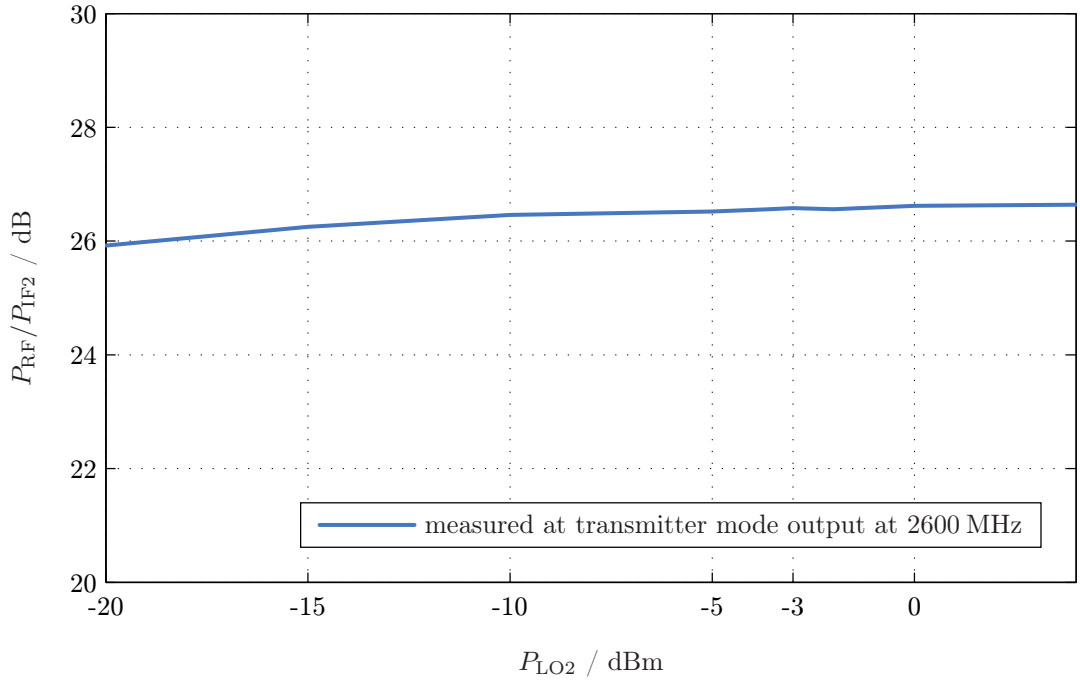

Figure 5.19: Conversion gain for the transmitter mode output of the "RF2600" section as a function of the LO2 input power.
$f_{IF2} = 947{,}5$ MHz, $P_{IF2} = -15$ dBm, $f_{LO2} = 1652{,}5$ MHz

5.5 Error Vector Magnitude

Since the transmitter is intended to be used with signals of different digital modulation schemes, measurements with such signals have been performed as well. Figure 5.20 gives the spectrum of one of those signals. It is a 64QAM[9] signal with a symbol rate *SR* of 20 MSymbl/s. As modulation filter a root raised cosine filter (RRC) with a shape factor $\alpha = 0{,}25$ was used. This results in a 3 dB bandwidth of approximately 20 MHz. The signal is generated by a VSG[10] at the second intermediate frequency f_{IF2} of 947,5 MHz, fed into the "RF2600" section, and received with a VSA[11]. This is illustrated in Figure 5.21 for a similar measurement taken on the complete transmitter. Figure 5.22 shows the received symbols after downconversion with the VSA in the base band and the ideal reference points of the constellation diagram.

Due to linear and nonlinear distortions as well as noise the received symbols are not located on the reference points any longer but shifted near another reference point. As illustrated in Figure 5.23 the symbol vector to the measured point M can be divided into a vector to the reference point R and an error vector. The

[9] Quadrature Amplitude Modulation with a symbol alphabet of 64
[10] Vector Signal Generator
[11] Vector Signal Analyzer

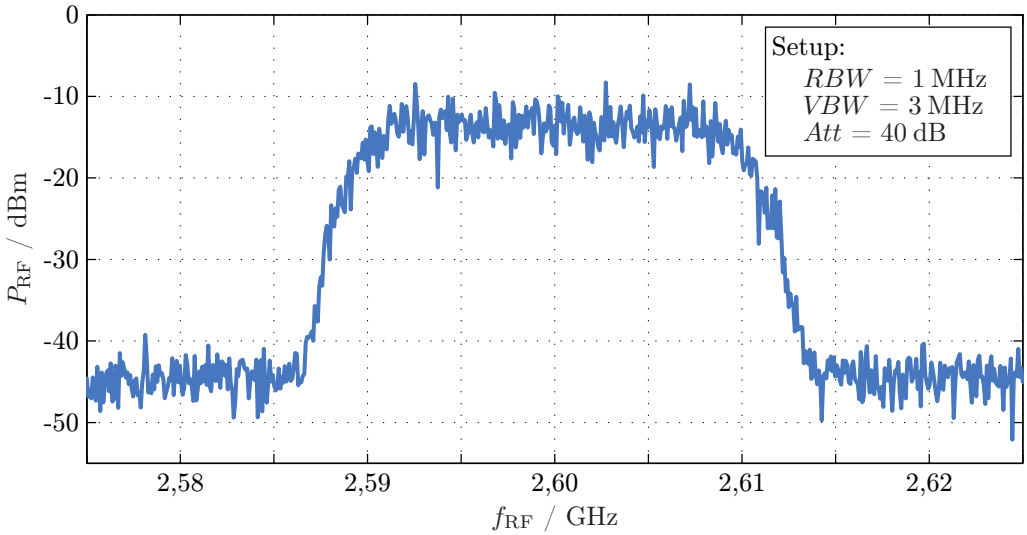

Figure 5.20: Spectrum of a 64QAM signal with 20 MSymbl/s and a root raised cosine filter with $\alpha = 0{,}25$.

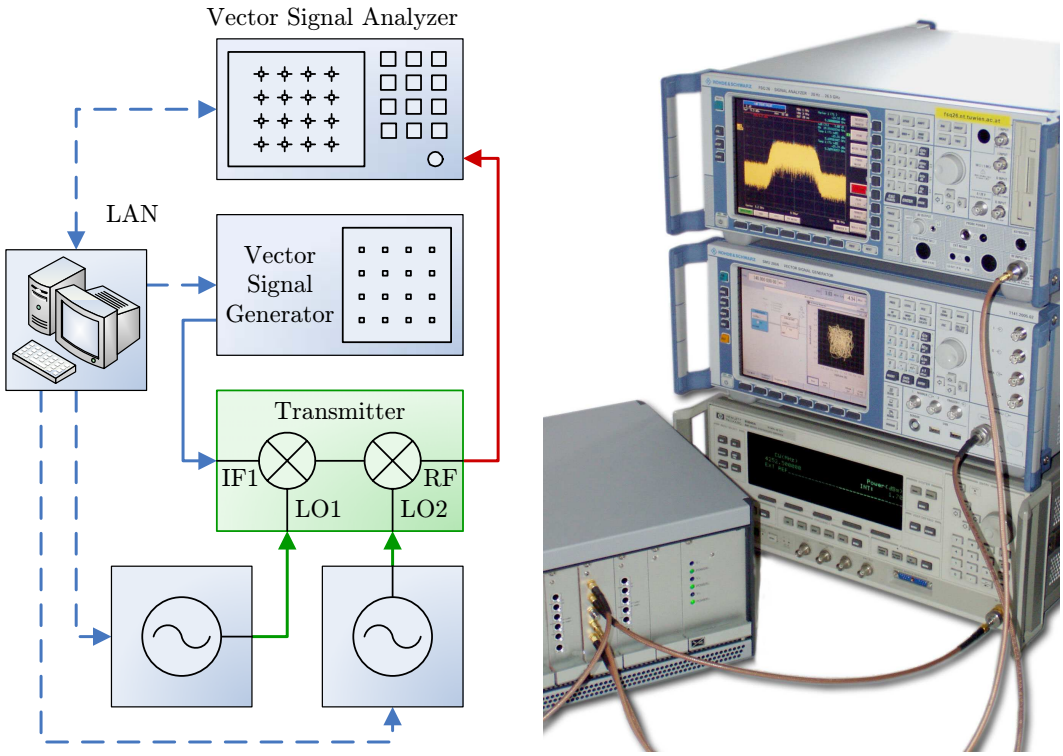

(a) (b)

Figure 5.21: Measurement setup for EVM measurements.

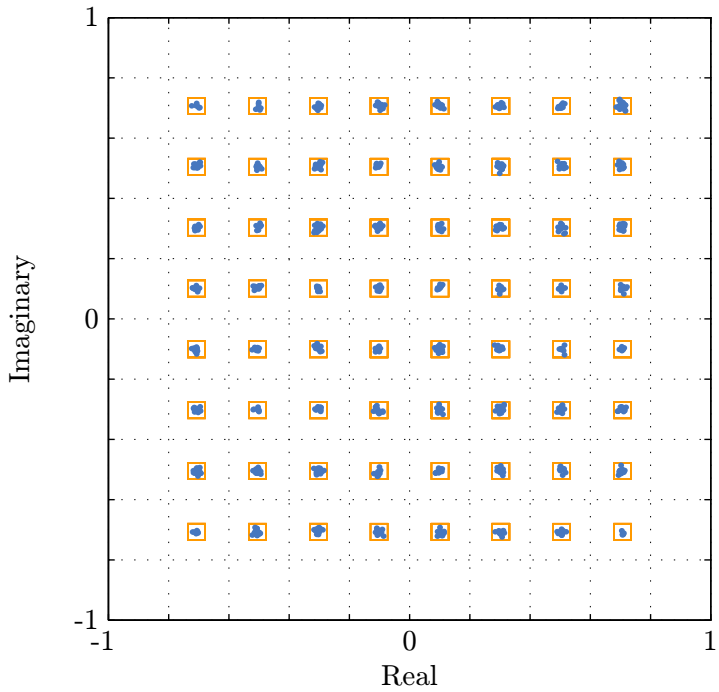

Figure 5.22: Received symbols and reference points during 64QAM.

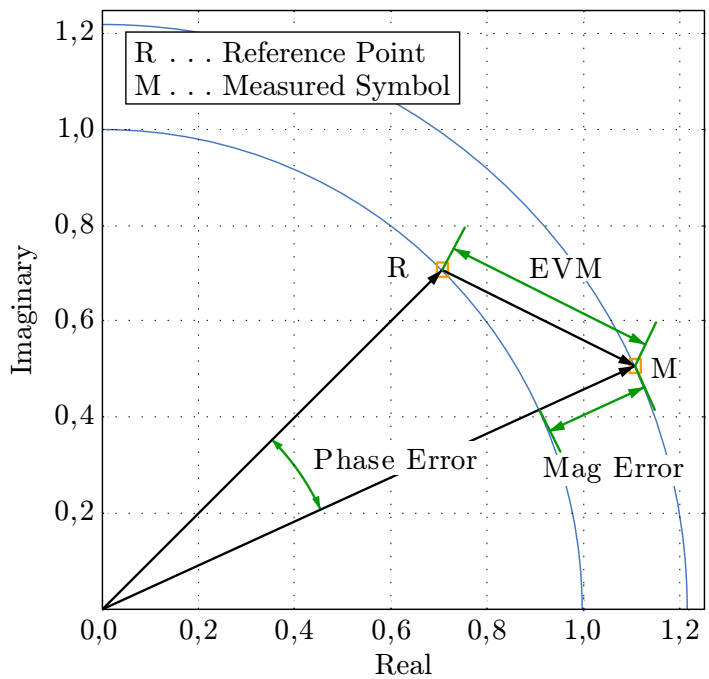

Figure 5.23: Definition of the error vector magnitude ([22] ch. 3, p. 3-52).

magnitude of this error vector is called EVM[12] and is an integral measure for those different kinds of distortions (see [22] ch. 3 and ch. 9.1).

$$EVM = \frac{|M - R|}{C} \ , \tag{5.2}$$

with

$$C = \sqrt{\frac{1}{K} \sum_{K} |R_k|^2} \ . \tag{5.3}$$

Several automated measurements have been taken with variation of different parameters. Figure 5.24 shows the EVM as a function of input power. The input power is denoted as the RMS power level of the input signal on the horizontal axis. Since the crest factor CF of these signals is between 6,7 and 7,3 dB the PEP[13] is higher by this value. At input powers below −40 dBm the input signal to the VSA is too low for proper demodulation. This has been shown by directly connecting the VSG to the VSA and taking measurements of this back-to-back setup. As the input power reaches −10 dBm the EVM degrades because of compression and saturation of the "RF2600" section. This is no problem since this is no longer the specified operation range. There is almost no variation with the size of the used symbol alphabet which has been verified with 16QAM and 32QAM signals. However the EVM is heavily dependant on the symbol rate and accordingly on the bandwidth of the signal. The ripple in the plots for signals with higher bandwidth in the medium power range is due to the suboptimal attenuator settings of the VSA. The results for the test mode output are compared to the transmitter mode output in Figure 5.25.

In order to compensate for linear distortions due to e.g. the non-ideal frequency response of the "RF2600" section, an equalizer in the VSA (i.e. the receiver) has been used. As can be seen in Figure 5.26 the same results as for signals with SR = 1 MSymbl/s can be achieved for signals with SR = 20 MSymbl/s. However the training of the equalizer of the VSA only works at high power levels. The equalizer can be implemented as a digital predistortion filter before the transmitter in the digital baseband processing unit, thus resulting in fine output performance.

Last but not least Figure 5.27 shows the EVM as a function of the symbol rate. Again it can be seen that using an equalizer to remove linear distortions almost nullifies the impact of higher bandwidths.

[12]Error Vector Magnitude
[13]Peak Envelope Power

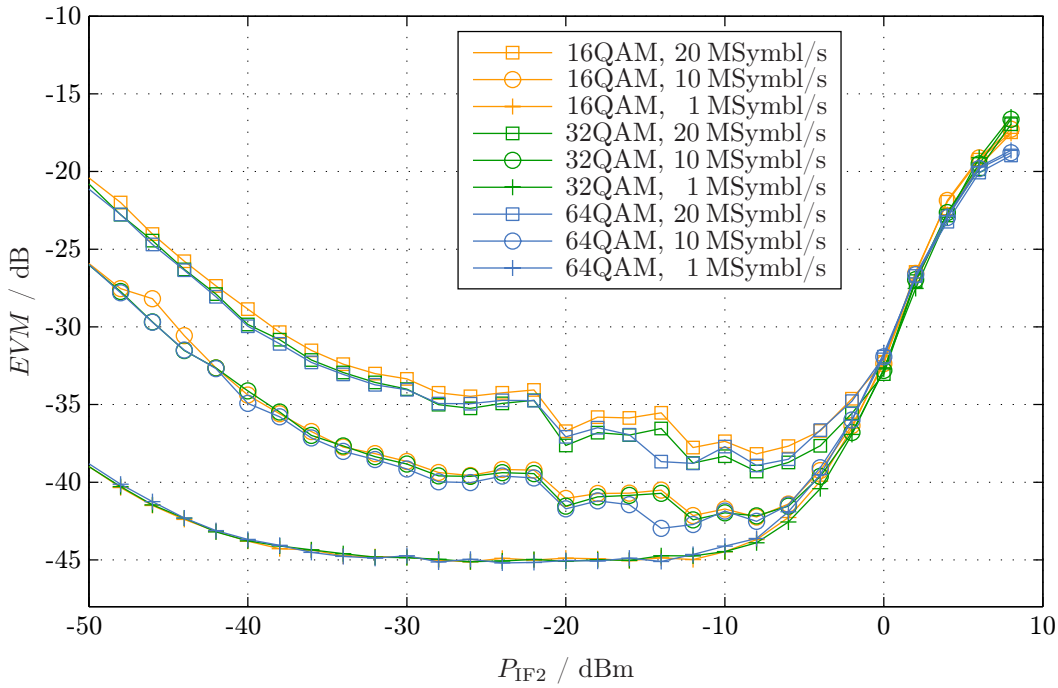

Figure 5.24: EVM as a function of input power, modulation scheme, and symbol rate.

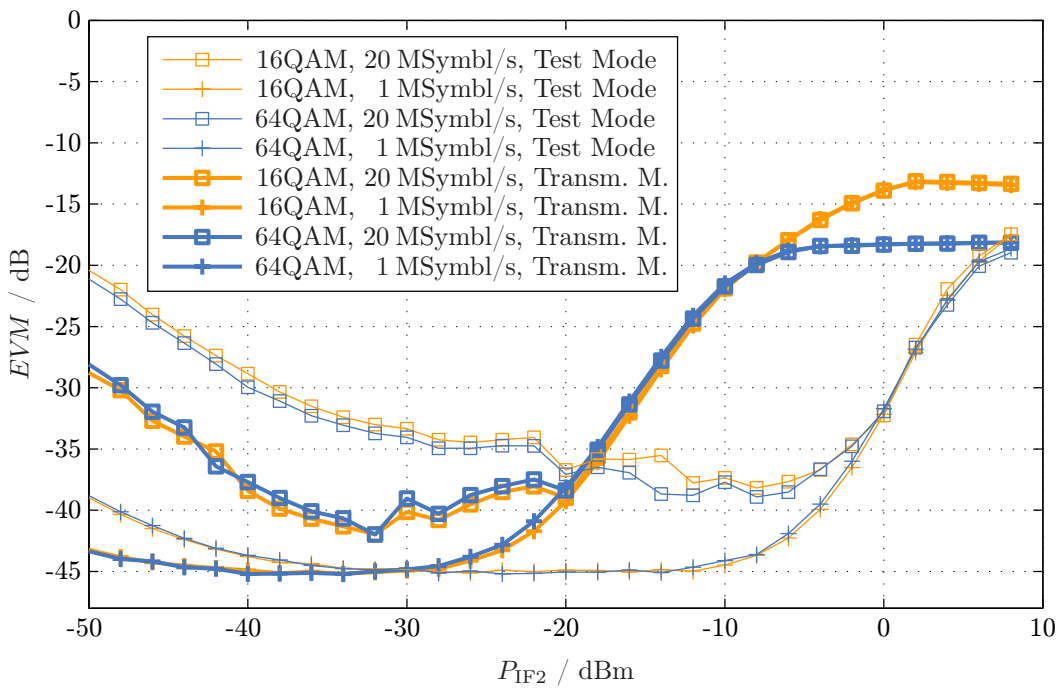

Figure 5.25: Comparison of EVM for transmitter and test mode output as a function of input power, modulation scheme, and symbol rate.

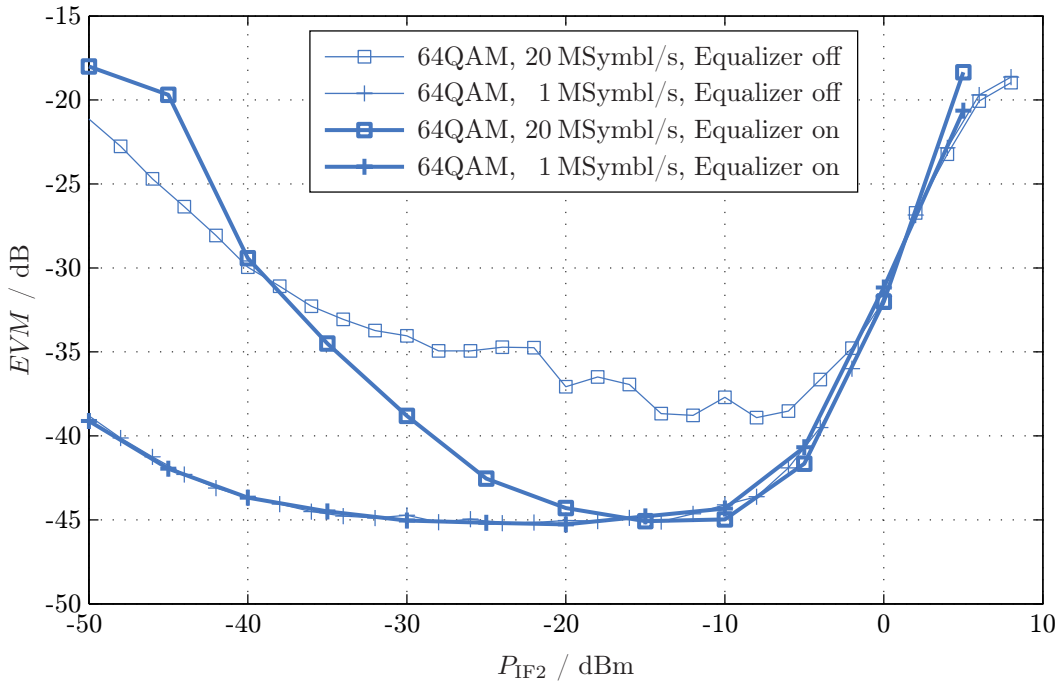

Figure 5.26: EVM as a function of input power, equalizer setting, and symbol rate.

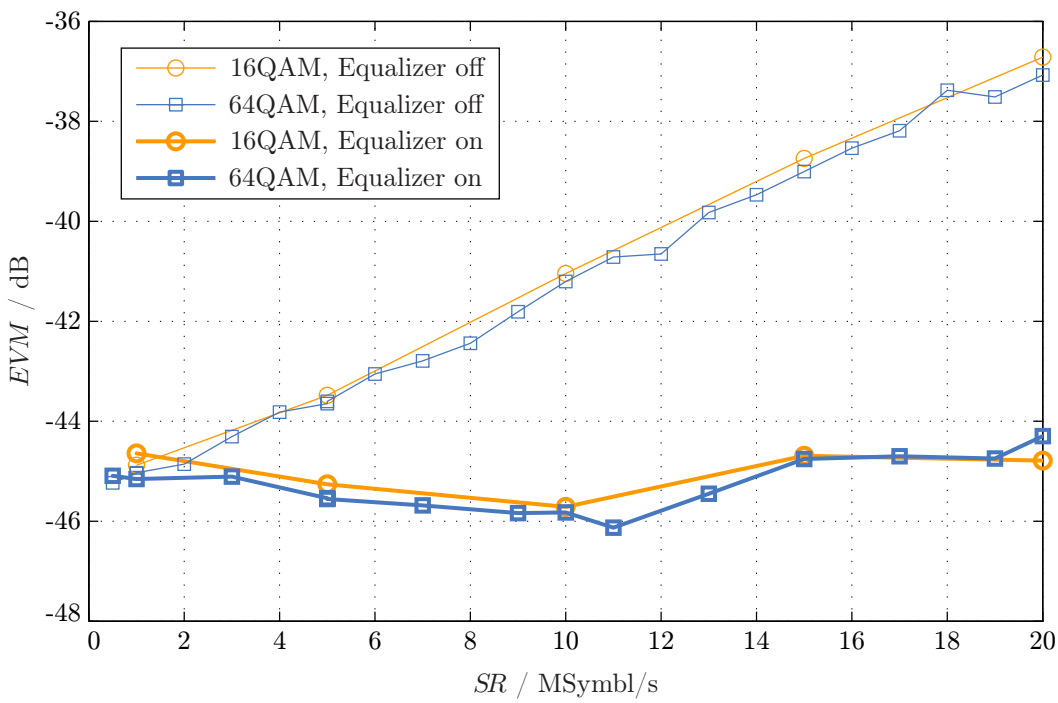

Figure 5.27: EVM as a function of symbol rate (i.e. bandwidth), equalizer settings, and modulation scheme.

Chapter 6

Summary

In this diploma thesis I first described possible scenarios in which a flexible RF front end is required. I further extended these situations to MIMO applications. This leads to the requirements for such a front end. The RF front end consists of transmitter, receiver and local oscillators. All are designed in a modular way to allow for easy expansion or replacement. Only one local oscillator unit is used for multiple transmitters or receivers for easy synchronization in MIMO applications.

The main work of this diploma thesis has been the transmitter and especially the "RF2600" section. After research and simulation, each component of the "RF2600" section has been built up on a test PCB and characterized. The results have been given in Chapter 4.

Next all components of the "RF2600" section have been prepared for the combination on a single PCB. Layouts for a double sided PCB and two solder mask layers have been generated. With those the PCB has been manufactured by an external company. The components and PCB have been assembled and put into operation. It can be mounted atop the base PCB. This is shown in Figure 6.1.

To evaluate the performance of the transmitter, different measurements have been performed. They describe the behavior in the frequency domain and at different power levels. Furthermore they show that the transmitter fulfills its specifications.

When accompanied with the receiver, the transmitter – as the RF front end – augments the baseband processing unit to a flexible and powerful instrument for a multitude of purposes. The "RF2600" section can be used as a guideline to design additional RF sections for different output frequency bands if required.

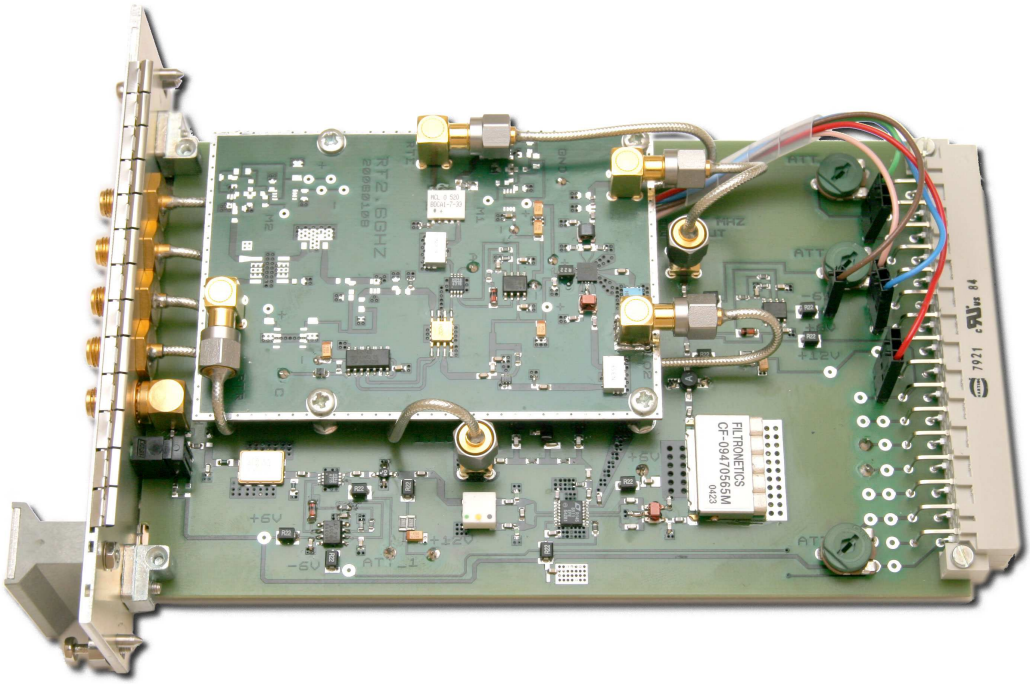

Figure 6.1: Photo of the transmitter for 2,6 GHz.

Acknowledgments

I would like to thank my supervisors Robert Langwieser and Arpad L. Scholtz for their guidance and support throughout this diploma thesis.

I would also like to thank my friends and my colleagues from university for their encouragement and help during my studies.

But above all I would like to thank my family. This work would not have been achievable nor possible without their support.

Bibliography

[1] David M. Pozar, *Microwave engineering*, Addison-Wesley Publishing Company, Inc., 1991

[2] K.C. Gupta, Ramesh Garg, I.J. Bahl, *Microstrip Lines and Slotlines*, Artech House, Inc., Dedham (Massachusetts), 1979

[3] Reinmut K. Hoffmann, *Integrierte Mikrowellenschaltungen*, Springer, Berlin, 1983

[4] Otto Zinke, Heinrich Brunswig, *Hochfrequenztechnik 1*, Herausgeber A. Vlcek, H.L. Hartnagel, K. Mayer, 6. Auflage, Springer Lehrbuch, Berlin, 2000

[5] Otto Zinke, Heinrich Brunswig, *Hochfrequenztechnik 2*, Herausgeber A. Vlcek, H.L. Hartnagel, K. Mayer, 5. Auflage, Springer Lehrbuch, Berlin, 1999

[6] Linear Technology, *LT5521 Very High Linearity Active Mixer*, data sheet `http://www.linear.com/pc/downloadDocument.do?navId=H0,C1,C1011,C1723,P2506,D3107`

[7] NTK, *MFE2593CCF21 – Dielectric Filter with Attenuation Pole*, data sheet `http://www.ntktech.com/DF_Duplexer/DF_Duplexer_PDF/MFE2593CCF21.pdf`

[8] Trans-Tech, *CRaFT 1.1a – Ceramic Resonator Filter Tool*, `http://www.trans-techinc.com/craftprogramform.cfm`

[9] UBE Electronics, Ltd., *The Filter Simulator Fuji-Yama for Dielectric Ceramic Filters*, `http://www.uel.co.jp/sim/sim.html`

[10] Agilent Technologies, *MGA 61563 – Current Adjustable, Low Noise Amplifier*, data sheet `http://www.avagotech.com/pc/downloadDocument.do?id=4891`

[11] Hittite, *HMC232G8 – GaAs MMIC High Isolation SMT SPDT Switch, DC - 6.0 GHz*, data sheet `http://www.hittite.com/product_info/product_specs/switches/hmc232g8.pdf`

[12] Agilent Technologies, *MGA 83563 – +22 dBm 3 V GaAs Power Amplifier for 0.5 - 6 GHz Applications*, data sheet `http://www.avagotech.com/pc/downloadDocument.do?id=5499`

[13] Mini-Circuits, *Bi-Directional Couplers*, catalogue brochure
`http://www.minicircuits.com/dg03-192A.pdf`

[14] Agilent Technologies, *Agilent HSMS-286x Series Surface Mount Microwave Schottky Detector Diodes*, data sheet
`http://www.avagotech.com/pc/downloadDocument.do?id=5363`

[15] Raymond W. Waugh, "Designing Large-Signal Detectors for Handsets and Base Stations", *Wireless Systems Design*, Vol. 2, No. 7, July 1997, pp 42-48

[16] Hittite, *HMC346MG8G – GaAs MMIC SMT Voltage-Variable Attenuator, DC - 8 GHz*
`http://www.hittite.com/product_info/product_specs/attenuators/hmc346ms8g.pdf`

[17] Matlab, *The Language of Technical Computing*, MathWorks, 1984-2006

[18] R. Hajji, F, Beanregard, F.M. Ghannouchi, "Multitone power and intermodulation load-pull characterization of microwave transistors suitable for linear SSPA's design", *IEEE Transactions on Microwave Theory and Techniques*, Vol. 45, No. 7, pp.1093-1099, July 1997

[19] J.C. Pedro, N.B. De Carvalho, "On the use of multitone techniques for assessing RF components' intermodulation distortion", *IEEE Transactions on Microwave Theory and Techniques*, Vol. 47, No. 12, pp. 2393-2402, December 1999

[20] K.A. Remley, "Multisine excitation for ACPR measurements", *2003 IEEE MTT-S International Microwave Symposium Digest*, Vol. 3, pp. 2141-2144, 8-13 June 2003

[21] H. Boche, G. Reissig, "Behavior of multitone signals with Schroeder's phase" *1998 Fourth International Conference on Signal Processing Proceedings*, Vol. 1, pp. 133-136, 1998

[22] Rohde&Schwarz, "Applications Firmware R&S FSQ-K70", *Vector Signal Analysis*, Software Manual, January 2006

List of Abbreviations

ADC	Analogue to Digital Converter
BALUN	BALanced - UNbalanced converter
BPF	Band Pass Filter
DAC	Digital to Analogue Converter
DC	Direct Current
DSP	Digital Signal Processor
DUT	Device Under Test
FPGA	Field-Programmable Gate Array
GPIB	General Purpose Interface Bus (IEEE 488)
HPF	High Pass Filter
IF	Intermediate Frequency
LAN	Local Area Network
LED	Light Emitting Diode
LO	Local Oscillator
LPF	Low Pass Filter
MIMO	Multiple Input Multiple Output
PCB	Printed Circuit Board
64QAM	Quadrature Amplitude Modulation with a symbol alphabet of 64
RF	Radio Frequency
RMS	Root Mean Square
RRC	Root Raised Cosine
SMA	SubMiniature version A (connector)
SNR	Signal Noise Ratio
VNA	Vector Network Analyzer
VSA	Vector Signal Analyzer
VSG	Vector Signal Generator

List of Symbols

$ACPR$	Adjacent Channel Power Ratio
Att	Attenuator Level
BW	Bandwidth
$CCPR$	Co-Channel Power Ratio
CF	Crest Factor
$\tan\delta$	Dielectric Loss Tangent
ε_r	Relative Permittivity
EVM	Error Vector Magnitude
f_c	Center Frequency
F	Noise Figure
G	Gain
g	Normalized Conductance
h	Thickness, Height
IP_3	3rd Order Intercept Point
P	Power
$P_{1\text{dB}}$	1 dB Compression Point
PEP	Peak Envelope Power
ϱ	Reflection Coefficient
RBW	Resolution Bandwidth (of Spectrum Analyzer)
SR	Symbol Rate
U	Voltage
VBW	Video Bandwidth (of Spectrum Analyzer)
w	Width
Z	Complex Impedance
z	Normalized Complex Impedance
Z_w	Characteristic Impedance of Transmission Line
Z_0	Characteristic Impedance of System

List of Figures

1.1 Typical telecommunication scenario 1

2.1 The RF front end used for channel sounding 3
2.2 The RF front end used for channel emulation 4
2.3 The RF front end used for test measurements 5
2.4 The RF front end used in MIMO applications 6
2.5 The complete system 7
2.6 The complete baseband processing unit 7

3.1 Overview of the transmitter components 11
3.2 Block diagram of the transmitter 12
3.3 Specification of the transmitter 12
3.4 Spectral overview of the transmitter 13
3.5 Parameters of microstrip lines 15

4.1 Overview of the “RF2600” section 16
4.2 Specification of the “RF2600” section 17
4.3 Power level diagram for the “RF2600” section 19
4.4 Overview of the second upconverter stage 20
4.5 Layout with part outlines and assembled test PCB of the mixer . 21
4.6 Frequency response of the NTK MFE2593CCF21 filter 22
4.7 Schematic of the buffer amplifier 23
4.8 Smith Chart of the input matching network for the buffer amplifier 24
4.9 Input match and gain of the buffer amplifier 24
4.10 Schematic and layout with part outlines of the RF switch 26
4.11 Overview of the transmitter mode output branch 26
4.12 Layout and assembled test PCB of the power detector 29
4.13 Output voltage as a function of input power for the power detector 30
4.14 Overview of the test mode output branch 31
4.15 Schematic of the variable attenuator 32
4.16 Layout and part outlines of the variable attenuator 32
4.17 Complete layout and part outlines of the “RF2600” section 34
4.18 Photo of the “RF2600” section PCB 34

5.1 Block diagram of the setup for measuring the frequency response of the complete transmitter 36
5.2 Photo of the setup used for measuring the complete transmitter . 36

5.3 Frequency response of the "RF2600" section as a function of the input frequency . . . 37
5.4 Frequency response of the "RF2600" section as a function of the second local oscillator frequency for the test mode output . . . 37
5.5 Frequency response of the complete transmitter . . . 38
5.6 Full concatenated frequency response of the complete transmitter 39
5.7 Variation of the conversion gain of the complete transmitter as a function of the LO2 frequency and the IF1 bandwidth . . . 39
5.8 Output power as a function of input power for the "RF2600" section PCB measured at the transmitter mode output . . . 41
5.9 Gain of the "RF2600" section PCB as a function of input power . 41
5.10 Traditional two-tone setup for intermodulation measurements . . 42
5.11 Input and output signals for the two-tone intermodulation measurement of the "RF2600" section . . . 43
5.12 Power of the intermodulation products for the test mode output of the "RF2600" section . . . 44
5.13 Power of the intermodulation products for the transmitter mode output of the "RF2600" section . . . 45
5.14 Versatile setup for measurements with double and multi beat signals 45
5.15 Spectrum of the multi beat signal at different input levels . . . 46
5.16 *ACPR* and *CCPR* as a function of the input power for the "RF2600" section . . . 47
5.17 Overview of the output of the "RF2600" section . . . 48
5.18 Power of the 3rd harmonics of LO2 at the test mode output as a function of the LO2 input power . . . 49
5.19 Conversion gain for the transmitter mode output of the "RF2600" section as a function of the LO2 input power . . . 50
5.20 Spectrum of a 64QAM signal . . . 51
5.21 Measurement setup for EVM measurements . . . 51
5.22 Received symbols and reference points during 64QAM . . . 52
5.23 Definition of the error vector magnitude . . . 52
5.24 EVM as a function of input power, modulation scheme, and symbol rate . . . 54
5.25 Comparison of EVM for transmitter and test mode output as a function of input power, modulation scheme, and symbol rate . . 54
5.26 EVM as a function of input power, equalizer setting, and symbol rate . . . 55
5.27 EVM as a function of symbol rate, equalizer settings, and modulation scheme . . . 55

6.1 Photo of the transmitter for 2,6 GHz . . . 57

List of Tables

3.1 Parameters of the PCB substrate FR4 15

4.1 Power level plan for the “RF2600” section 18
4.2 Specification of the switch 25
4.3 Specification of the power amplifier 27
4.4 Power level plan for the test mode branch of the “RF2600” section 31

5.1 Conversion gain and its variation at various LO2 frequencies f_{LO2} and measurement bandwidths BW for the complete transmitter . 40
5.2 Intercept points of 3rd and 5th order for the transmitter and test mode outputs 44